GENERATION AND CHARACTERIZATION OF HEN EGG WHITE LYSOZYME AMYLOID VARIANTS

Nalla Lakshmi Prasanna

BO12M1002

A Dissertation Submitted to

Indian Institute of Technology Hyderabad

In Partial Fulfillment of the Requirements for

The Degree of Master of Technology

भारतीय प्रौद्योगिकी संस्थान हैदराबाद
Indian Institute of Technology Hyderabad

Department of Biotechnology

June, 2014

Declaration

I declare that this written submission represents my ideas in my own words, and where others' ideas or words have been included, I have adequately cited and referenced the original sources. I also declare that I have adhered to all principles of academic honesty and integrity and have not misrepresented or fabricated or falsified any idea/data/fact/source in my submission. I understand that any violation of the above will be a cause for disciplinary action by the Institute and can also evoke penal action from the sources that have thus not been properly cited, or from whom proper permission has not been taken when needed.

Prasanna

Nalla Lakshmi Prasanna

B012M1002

Approval Sheet

This thesis entitled **"Generation and Characterization of Hen Egg White Lysozyme Amyloid Variants"** by Nalla Lakshmi Prasanna is approved for the degree of Master of Technology from IIT Hyderabad.
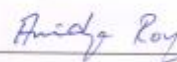
Dr. Basant Kumar Patel

(Thesis Advisor)

Department of Biotechnology

IIT Hyderabad

Dr.Parag D. Pawar

Department of Chemical Engineering

IIT Hyderabad

Dr. Anindya Roy

Department of Biotechnology

IIT Hyderabad

Dr. Thenmalarchelvi Rathinavelan

Department of Biotechnology

IIT Hyderabad

Acknowledgement

I would like to convey my gratitude to all individuals who have helped me with their kind support. I would also like to extend my sincere thanks to all of them.

I am highly indebted to my advisor Dr. Basant Kumar Patel, Department of Biotechnology, IIT Hyderabad for his guidance, providing necessary information regarding the project and also for his support in completing the project. I would like to express my gratitude towards the committee members and also my parents for their kind co-operation and encouragement which helped me in completion of this project.

Furthermore, I would like to express my special gratitude and thanks to my lab mates S. Vishwanath, Neethu Sharma and Archana Prasad for giving me support for executing the project. Thank you everyone once again for your great support for the successful completion of my project.

Contents

ABBREVIATIONS

GdnHCl: Guanidine Hydrochloride

HEWL: Hen Egg White Lysozyme

ThT: Thioflavin T

CR: Congo Red

PBS: Phosphate Buffered Saline

ANS: 1-anilinonaphthalene-8-sulfonate

Trp: Tryptophan

SDD-AGE: Semi Denaturing Detergent Agarose Gel Electrophoresis

SDS: Sodium Dodecyl Sulphate

PVDF: Polyvinylidene difluoride

BSA: Bovine Serum Albumin

HSA: Human Serum Albumin

ABSTRACT

There are numerous proteins that are found capable of forming beta sheet-rich aggregates called as amyloid aggregates. Amyloid- like aggregates is seen in wide range of diseases such as Alzheimer's disease, Parkinson's disease, Prion disease and diabetes etc. Amyloid aggregates of prion diseases have the distinction of being infectious.

Astonishingly, a single polypeptide of a prion protein can fold into different amyloid conformations which differ in structural features and yield faithfully propagating prion strains or variants that manifest as different symptoms of the disease. One key question, therefore, is whether the ability to form variants is limited to a prion protein or a general property of all amyloids. In this regard, it was investigated here whether the amyloid forming protein hen egg white lysozyme (HEWL) could form amyloid variants. Indeed we have found that by altering the fibrillization conditions, it is possible to obtain HEWL amyloid variants. These findings could have implications in understanding of the human lysozyme amyloidosis disease affecting kidney which is found to be associated with different hereditary mutation in lysozyme in different subjects. Furthermore, the findings here support that amyloid variant formation may be a generic property of amyloid forming proteins.

CHAPTER I

REVIEW OF LITERATURE

1.1. INTRODUCTION

The name 'amyloid' was coined initially by Rudolph Virchow in 1954. The deposits found in kidney liver and spleen of diseases patients were given the name amyloid based on the color reaction with iodine and sulphuric acid similar to starch (amylum) [1]. But now we know that those deposits called amyloids are actually beta sheet rich protein aggregates and many proteins have the inherent property of forming amyloid-like aggregates [2].

Interest in studying amyloid fibrils stems from their participation in different fields such as their role in diseases [3, 4], role as an alternative structural state for many peptides and proteins [5]. Almost all polypeptides can form amyloid under appropriate conditions and the process of such conversion has become a central question in protein biochemistry [3]. Amyloids can also be used as basis for nanomaterials with possible applications [6].

Amyloids are associated with number of diseases such as Alzheimers, Parkinsons and prion diseases. Moreover it is also found that few amyloids have a particular role in normal biology. These amyloids are termed as functional amyloids [3, 7]. Structural studies on amyloid were initially done by investigating the X-ray diffraction patterns [8]. It was concluded that there are elongated peptide chains arranged parallel to each other but perpendicular to the axis of the aggregate (amyloid finer). This is referred as cross-beta structural pattern [9] **(Figure 1.1)**.
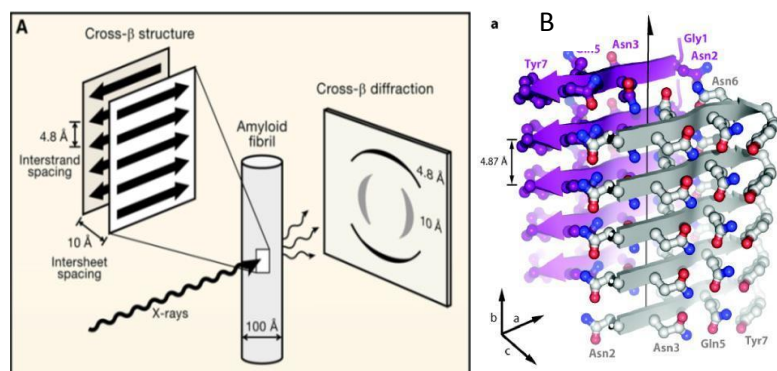

Figure 1.1 (a) Cross beta diffraction pattern as observed when focused by X-rays. (David Eisenberg, et al. Cell, 2012, [4]). (b) Cross-beta sheet structure of the segment GNNQQNY from yeast prion protein Sup35 with central fibril axis. (Nelson R, et al. Nature, 2005, [10]).

1.2. AMYLOID

Amyloid is an abnormal protein, insoluble in nature, fibrous, cross beta sheet containing extracellular proteinaceous deposit found in tissues and organs in vivo [11].

The route of amyloid formation involves partial unfolding of polypeptides chains resulting in a conformation which enables the polypeptide chains to interact with each other and organize into an ordered structure called amyloid fibrils. These are beta sheet rich protein deposits; they show cross beta diffraction pattern. The beta sheets run parallel to the fiber axis with individual beta strands perpendicular to the fiber axis [10]. Amyloids exhibit a phenomenon known as seeding i.e. the rate of formation of fibrils by amyloidogenic protein increases by the addition of preformed fibrils [12]. Amyloids are long, unbranched, filamentous, insoluble, and protease resistant fibrils. Their diameter varies from 80-100 A° and length from 1000-16000 A° (**Figure 1.2**).
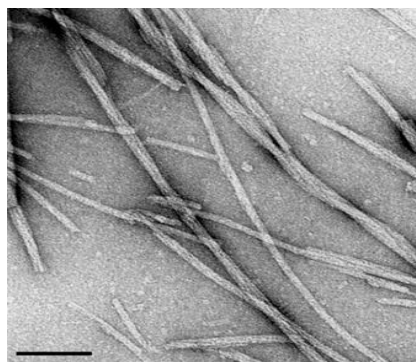
Figure 1.2: Electron micrographic view of amyloid fibrils

Asparagine and glutamine are commonly found in amyloid structures, they bind to dyes like thioflavin T resulting in enhanced fluorescence and Congo red resulting in apple green birefringence. These features differentiate the amyloid fibrils from other fibril like structures such as silk fibroin and collagen. Amyloids also exhibit partial stability against denaturants like Guanidine Hydrochloride (GdnHCl) and non-specific proteases like proteinase K. Different proteins can be deposited extracellular as amyloid in various locations of human body.

The growth of amyloid occurs mostly via nucleation dependent polymerization process (**Figure 1.3**). It shows a sigmoidal growth curve which includes three phases: Lag

11

phase, log phase and stationary phase. In the presence of nucleus from preformed fibrils the amyloid growth occurs fast with reduced lag phase and the phenomenon is called seeding. Seeding can be done for same proteins called self-seeding. Seeding is also possible in closely related proteins sharing sequence similarity called cross-seeding. The seeding phenomenon is one of the important features of amyloid exhibited by almost all amyloid fibrils.
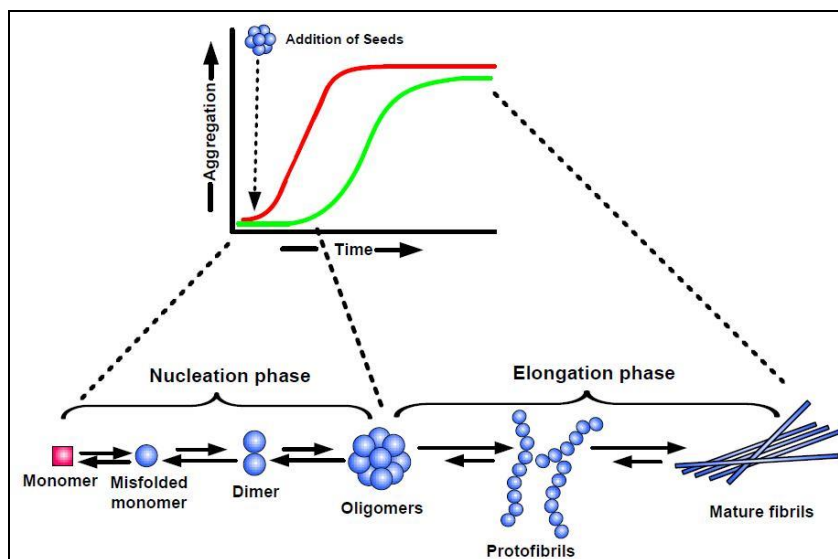
Figure 1.3: Nucleus formation and polymerization of amyloid fibrils [13].

With the understanding of amyloid structure, it has been found that single polypeptide can fold into different amyloid conformations as in case of prions [14, 15]. In this thesis, conformational variants of amyloid formed from a globular protein, lysozyme has been characterized. The protein was fibrillized *in vitro* under different physiological conditions and then assessed for the conformational variants.

1.3. AMYLOIDOSIS

Amyloidosis is a class of diseases associated with the deposition of abnormally folded proteins in the form of amyloid fibrils. In few cases called Familial or primary amyloidosis, amyloid fibrils result due to the presence of abnormal protein. The major cause of amyloid deposits associated with disease in vivo is the point mutation in the amino acid sequence which destabilizes the protein. In other cases called senile

amyloidosis, amyloid deposits occur due to abnormally high quantity of protein or due to its presence for many years [1]. The amyloid deposits restricted to a particular organ lead to localized amyloidosis, example: Aβ amyloidosis (Alzheimer disease) and amyloid deposits affecting many different organ systems lead to systemic amyloidosis, example: AL amyloidosis (immunoglobulin light chain) [16]. The modern classification of amyloid protein was decided at the Second International Symposium on Amyloidosis, Helsinki (1974). Some of the amyloid diseases and their respective amyloid proteins are listed below in the **table 1.1**.

Table 1.1: Amyloid diseases and their precursor proteins [5]

S. No.	Amyloid Diseases	Amyloid protein
1	Alzheimer's disease	Amyloid β peptides
2	Parkinson's disease	α-synuclein
3	Huntington's disease	Huntingtin
4	Primary systemic amyloidosis	Immunoglobulin light and heavy chains
5	Atherosclerosis	Apolipoprotein AI
6	Atrial amyloidosis	Atrial natriuretic factor
7	Rheumatoid arthritis	Serum amyloid A
8	Familial amyloid polyneuropathy	Transthyretin
9	Hereditary non-neuropathic systemic amyloidosis	Lysozyme
10	Dialysis related amyloidosis	β-2 microglobulin

1.4. PRIONS

Prion diseases or transmissible spongiform encephalopathies are neurodegenerative disorders seen in both humans and animals. The causative agents are believed to be prion proteins. Prions are infectious protein, similar to virus but lack nucleic acid. They can propagate in misfolded state and can induce other properly folded proteins to misfold leading to amyloid plaque formation and neurodegeneration [17]. Prions are ordered cross-beta aggregates similar to amyloids. Several studies on prion structure, their transmission, mechanism of formation has been done using yeast models and yeast prion proteins. The normal prion protein PrP^c is converted to infectious conformational isoform PrP^{SC} in mammals [18]. They are called infectious since they can convert other PrP^c molecules to misfolded PrP^{SC} form. Several studies have shown that yeast contains proteins either in soluble form or in infectious amyloid form. Protein in soluble and infectious form shows different phenotype. Prion aggregates mostly results in "loss of function phenotype", example: Sup35 is translational termination factor in yeast which when converts to prion form results in less efficient translational termination. Not only loss of function prion forms can also result in "gain of new function". Example: [PIN+], prion forms of Rnq1enhances the formation of another prion *de novo*.

   Not only prions amyloids have also been hypothesized to form "functional amyloid". This hypothesis states that organisms have evolved to take advantage of such prion amyloid forms [7, 19]. **Table 1.2** below has enlisted few examples of functional amyloids.

In yeast each prion protein has been shown to form different infectious aggregates associated with different phenotype and different conformation. These are referred to as "prion variants". The rising number of prions and amyloid proteins reflects that they may have biological role.

Table 1.2: List of functional amyloids in different organisms

Organism	Protein	Function
Bacteria – *E. coli*	Curli	Help to create a proteinaceous matrix that enables surface adhesion and colony formation
Fungi – *Saccharomyces cerevisiae*	Ure2p	Regulates nitrogen metabolism
Fungi – *Podospora anserina*	HET-s	Regulates heterokaryon formation
Homo sapiens	Pmel17	Role in biosynthesis of the pigment melanin

1.5. VARIANTS OF PRIONS

Prion variants or strains can be defined as amyloids with different conformations of a single protein sequence and thus resulting in different phenotypes *in vivo*. All these variants can propagate successfully. For example, in yeast Sup35 protein results in [PSI+] prion protein. This [PSI+] prion forms different conformations of Sup35 [20-22]. Infections with these conformations lead to different prion strains. This finding solved a major question of how a protein- only infectious agent causes disease with different phenotypes in genetically identical animals. This kind of conformational variants can also be observed in amyloid aggregates.

So far, only few cases have been observed and Aβ11-25 amyloid is the best example. Different conformations of Aβ amyloid have been observed at different polymerizing conditions.

a) Aβ fibers form antiparallel structure at pH 7.4 as well as pH 2.4 but it was found that β-strand register was 17+k ⇔ 20−k at pH 7.4, and the register changed to 17+k ⇔ 22−k at pH 2.4 where k represents integer values, and the two numbers are the residue numbers of adjacent positions on neighboring β-strands [23].
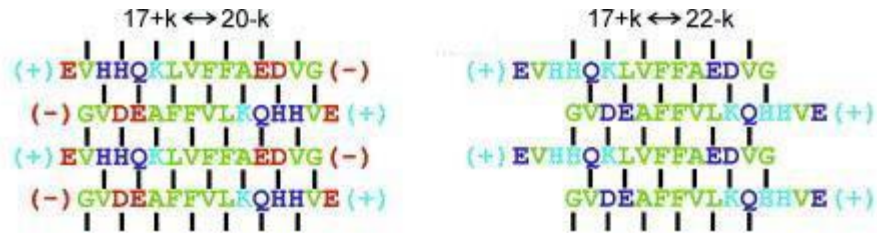
Figure 1.4: Different conformations of Aβ amyloid formed at different pH

Figure 1.4 shows the conformational variants formed at different pH conditions due to difference in secondary structure packing.

b) Full length Aβ1-40 peptide formed different amyloid structures under still and stirring conditions. Agitated fibers displayed two-fold symmetry i.e. two Aβ1–40 units per β-strand width, whereas the static fibers showed three-fold symmetry i.e. three Aβ1–40 units per β-strand width [24].

Two fold symmetry   Three fold symmetry
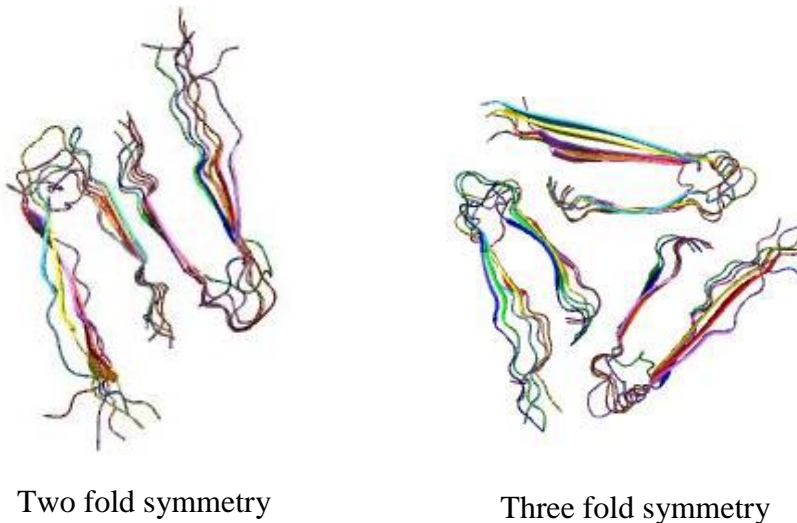
Figure 1.5: Two fold and three fold symmetry of amyloid formed from Aβ1-40 fragment

1.6. HEN EGG WHITE LYSOZYME: A MODEL AMYLOID

Here, we studied amyloid of the protein Hen Egg White Lysozyme (HEWL), which shares 60% sequence identity with human lysozyme. Natural variants of human lysozyme are known to form amyloid plaques *in vivo* resulting in familial non-neuropathic systemic amyloidosis. The protein lysozyme was discovered by Flemming in 1922. Since then lysozyme has served as a good model protein for investigations on protein structure and function. A wealth of information is available on the structural details and folding of both human and HEW lysozyme. Lysozyme has been isolated in human tears, saliva and mother's milk, as well as viruses, bacteria, phage, plants, insects, birds, reptiles and other mammalian fluids. It has a molecular weight of 14307 Da and is synthesized by hepatocytes, polymorphs and macrophages. It hydrolyzes β (1-4) linkages between N-acetylmuraminic acid and N-acetyl-D-glucosamine residues in peptidoglycan [25, 26].

HEWL forms amyloid fibrils *in vitro* under acidic conditions (pH 2.0, glycine HCl buffer) at 37 °C similar to the pathogenic fibrils of human lysozyme in physiological environment. Several other conditions have been developed for the fibrillization of hen egg white lysozyme which includes (a) incubation at elevated temperatures (60 °C) and low pH, 2.0, (b) incubating soluble lysozyme in concentrated solution of ethanol, (c) SDS (at very low concentrations) has also been found to induce amyloid formation from hen egg lysozyme (d) moderate concentrations of guanidine hydrochloride is also shown to induce amyloid formation from hen egg lysozyme (e) alkaline pH at room temperature.

Structure: It has two structural domains, an alpha domain composed of alpha helices and a beta domain composed of triple stranded antiparallel beta sheet and a 3_{10} helix near C-terminal. 3_{10} helices are slightly shorter in length than α-helices at approximately three residues per turn. The active site has two catalytic residues i.e. glutamate-35 and aspartate-52. A cleft formed near active site allows the binding of substrates i.e. bacterial cell wall components.

It has four disulphide bonds between cysteine residues 6:127, 30:115, 64:80, and 76:94 which act to stabilize the structure.
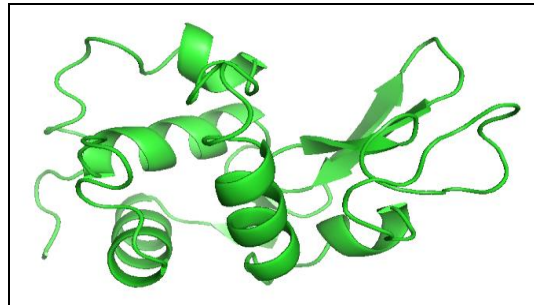
Figure 1.6: Structure of HEWL, PDB ID: 1HEW

Hen egg white lysozyme sequence (129 amino acids):

KVFGRCELAA AMKRHGLDNY RGYSLGNWVC AAKFESNFNT QATNRNTDGS TDYGILQINS RWWCNDGRTP GSRNLCNIPC SALLSSDITA SVNCAKKIVS DGNGMNAWVA WRNRCKGTDV QAWIRGCRL

Human lysozyme sequence (130 amino acids):

KVFERCELAR TLKRLGMDGY RGISLANWMC LAKWESGYNT RATNYNAGDR STDYGIFQIN SRYWCNDGKT PGAVNACHLS CSALLQDNIA DAVACAKRVV RDPQGIRAWV AWRNRCQNRD VRQYVQGCGV

1.7. LYSOZYME AMYLOIDOSIS

Human lysozyme is known to form amyloid fibrils similar to the pathogenic ones. Natural variants of human lysozyme are known to form amyloid plaques in vivo resulting in so called familial non-neuropathic systemic amyloidosis. The two common natural substitution mutations are Ile56Thr and Asp67His which cause autosomal dominant hereditary amyloidosis [27, 28]. The mutants are shown to be enzymatically active. Human lysozyme can cause growth of large quantities of amyloid in liver, kidney, and other regions of gastrointestinal tract leading to non-neuropathic systemic amyloidosis. Lysozyme amyloid mainly results in renal amyloidosis [29, 30]. Several studies have begun to find out the mechanism of how lysozyme aggregate *in vivo.*

Understanding the mechanism may help to come up with therapeutic implications for the treatment of lysozyme amyloidosis.

Table 1.3: List of mutations in human lysozyme leading to lysozyme amyloidosis

Mutation	Reported phenotype
Tyr54Asn	GI tract involvement Sicca syndrome
Ile56Thr	Renal failure, Petechiae
Phe57Ile	Renal failure
Trp64Arg	Renal failure, GI tract involvement Sicca syndrome, Spontaneous hepatic hemorrhage
Asp67His	Renal failure,GI tract involvement, Liver, Spleen,Sicca syndrome
Asp67Gly	Renal failure, Sicca syndrome
Trp112Arg	GI tract involvement, Liver, Spleen, Renal failure

From previous case reports it has been found that lysozyme amyloidosis results in recurrent hepatic hematoma [31]. Lysozyme amyloidosis has also been observed in association with sarcoidosis [32]. Other case reports show the renal manifestation with sicca syndrome, gastrointestinal symptoms and bleeding due to rupture of abdominal lymph nodes [29]. Thus lysozyme amyloidosis should be considered in cases of systemic amyloidosis with renal and gastrointestinal manifestations.

Lysozyme has been chosen as a working protein to look for the conformational variants formed under various conditions due to various reasons like lysozyme is a small ubiquitous protein and has been shown to form amyloid *in vitro* under various conditions. It is well characterized and its activity can be checked using *Micrococcus lysodeiktikus* bacterial cells. The enzymatic activity of lysozyme is a good tool to estimate the population of monomers and to check for the functionality once lysozyme is converted to amyloid. Natural mutants of human lysozyme lead to amyloidosis in humans affecting various organs. HEWL which shares good identity with human lysozyme has also been shown to form amyloid *in vitro* under certain destabilizing conditions. The enormous information available on lysozyme along with the various

conditions that have been successful in the aggregation of lysozyme *in vitro* makes lysozyme an ideal model for the study of amyloidosis.

1.8. BACKGROUND

From the initial observation of variants in amyloid formed from a single polypeptide there is similar possibilities of variants in other amyloid fibers and the consequence of these variants are now emerging as an important area of research. Different families suffering from lysozyme amyloidosis have resulted in different symptoms such as renal manifestations with sicca syndrome, gastrointestinal symptoms, and intense bleeding due to rupture of abdominal lymph nodes. This might be due to variants of human lysozyme carrying different mutations and thus showing different phenotype. Mark B. Pepys and his colleagues found that two families having similar gene mutation (Asp67His) were showing different phenotypes of lysozyme amyloidosis [33]. The reason for distinct phenotype is unknown however one possible reason could be different conformations of lysozyme amyloid.

Thus different conformations of lysozyme amyloid formed can be correlated with different phenotypes of lysozyme amyloidosis and also with previous studies on A-beta amyloid. Whether subtle changes could lead to changes in the rate of amyloid formation and conformation of aggregation will also be determined. With the two well-known natural mutants I56T and D67H of human lysozyme few more natural mutants have been discovered which cause lysozyme amyloidosis. They are F57I, W64R, T70N, W112R/T70N. The mutants can be analyzed for their conformational variants and thus correlating with different phenotype of lysozyme amyloidosis.
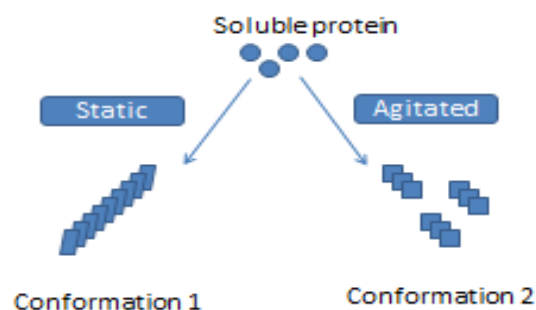

Figure 1.7: Different amyloid conformations expected to form under static and agitated conditions

CHAPTER II

MATERIALS AND METHODS

2.1. FORMATION OF HEN EGG WHITE LYSOZYME (HEWL) AMYLOID AGGREGATES

Amyloid aggregates were prepared at pH 2.0 by dissolving HEWL (Sigma, CAT no. L6876) in 0.5 M Glycine HCl buffer at a concentration of 1mM and incubating the solution at 37°C for 7 days [34]. Amyloid under different fibrillization conditions was formed by keeping agitation under one case and non-agitated in the other case. Non-agitated amyloid fibrils were formed at 37°C in the incubator whereas the agitated amyloid was formed in Spectra max M5e reader with agitation of 30 seconds after every 3 minutes.

Fibrillization buffer: Glycine-HCl buffer – 0.5 M

Working protein: HEWL – 1mM, Molecular weight – 14307 KDa, Amount of lysozyme weighed – 14.307 mg. Weighed amount was dissolved in Glycine – HCl buffer such that the final volume becomes 1ml.

2.2. CONFIRMATORY ASSAYS FOR AMYLOIDS AGGREGATES

2.2.1. Thioflavin – T (ThT) binding assay

Method: Thioflavin T (ThT) is a fluorescent dye and is used as a "gold standard" for selectively identifying the amyloid fibrils *in vitro*. ThT binding assay is more a sensitive and convenient technique. The dye selectively binds to amyloid fibrils subsequently showing a dramatic increase in fluorescent brightness [35]. LeVine initially characterized the binding property of ThT to amyloid fibrils. ThT associates rapidly with aggregated fibril giving rise to a new excitation maximum at 450 nm and enhanced emission at 482 nm, as opposed to the 385 nm (ex) and 445 nm (em) of the free dye [36]. ThT binds to diverse amyloid fibrils composed of different amino acid sequences. Since all amyloid fibrils contains a common cross beta core structure, it is largely believed that surface of cross-beta forms binding sites for ThT. Khurana et al. hypothesized that hydrophobic interactions exists between the amyloid and ThT micelles resulting in enhanced emission fluorescence [37].
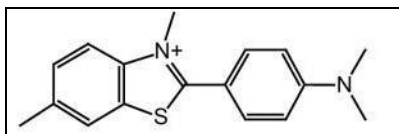
Figure 2.1: Structure of Thioflavin T

For testing the presence of lysozyme amyloid fibrils, an aliquote of 75 µl each from agitated and non-agitated samples incubated at 37°C for 7 days were mixed with 5 µl of 30 mM stock ThT. The mixture was stirred for one min in the 96- well microplate in the dark, after which the fluorescence was measured. A baseline measurement of just the ThT with fibrillization buffer was also taken. The fluorescence end point was recorded by excitation at 450 nm and observing the emission at 485 nm on a SpectraMax M5e fluorimeter. Excitation and emission spectra were also recorded.

For excitation spectra, emission was fixed at 485 nm and excitation spectra were scanned from 250 nm – 470 nm. For emission spectra, excitation was fixed at 450 nm and emission spectra were scanned from 460 nm – 560 nm.

Thioflavin - T stock: Initially a stock of ThT was made by dissolving 10 mg of ThT in 200 µl of dimethyl sulfoxide (DMSO). From this stock, 40 µl was taken and dissolved in 160 µl of distilled water to get a final concentration of 30mM.

2.2.2 Congo red (CR) binding assay

Congo red is a linear dye molecule and it is suggested that CR binds to amyloid by hydrogen bonds (amino group of congo red and hydroxyl groups of amyloid) and is simultaneously trapped in channels of beta pleated sheets by non-specific forces [38]. The binding of Congo red to amyloid induces a characteristic red shift in the maximal optical absorbance of the molecule from 490 nm to 540 nm. Congo red binding has been assumed to depend on the secondary, β-pleated configuration of the fibril, possibly mediated by hydrophobic interactions of the benzidine centers as well as the electrostatically charged terminal groups.
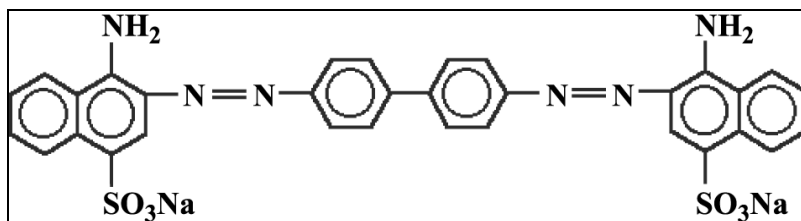
Figure 2.2: Structure of Congo red

For Congo red binding assay, a fresh stock solution of Congo red (from Himedia, CAT no. RM508) was prepared in phosphate buffered saline from sigma (PBS buffer, pH 7.4: NaCl – 0.137M, KCl – 2.7 Mm, KH_2PO_4 – 1.5 mM, Na_2HPO_4 – 8.1 mM) with 10% ethanol to avoid micelle formation. The lysozyme amyloid sample of 1mM was diluted three times to get a final concentration of 0.33 mM (330 μM). To this, Congo red was added from the stock to get the final concentration of 32 μM thus bringing the protein to CR ratio nearly 10: 1. Spectrophotometric analysis of CR-lysozyme amyloid binding was performed using Spectra max M5e spectrofluorimeter. Absorption spectrum was recorded from 300 nm to 700 nm range. CR-Lysozyme amyloid mixture was incubated for thirty minutes before spectral analysis.

Congo red stock: A stock of 10 mM of Congo red was prepared in PBS buffer with 10 % to avoid micelle formation. From the above stock another stock of 100 μM was prepared to use in the assay.

2.3. MEASUREMENT OF TURBIDITY BY LIGHT SCATTERING

After confirming that the aggregates formed are amyloid like aggregates but not amorphous aggregates, light scattering assay was performed to throw light on the size of the particles. Particles present in solution scatter the incident light and fluctuations in the scattered light intensity is based on particle size. Light scattering was measured at both excitation and emission wavelength of 450 nm. This kind of scattering is called as Rayleigh scattering. The higher order amyloid aggregates are expected to show more scattering than the soluble protein.

In a 96 well-plate, an aliquot of 100 μl from 1mM solution of soluble lysozyme and amyloid fibrils formed under agitated and non-agitated conditions were taken. The samples incubated along with ThT were used in this assay to measure the scattering.

The light scattering was measured by setting both the excitation and emission wavelength to 450 nm in spectra max spectrofluorimeter. Scattering of respective blanks were also measured.

2.4 ANALYSIS OF HYDROPHOBIC REGIONS OF HEWL AMYLOID FORMED UNDER STATIC VS AGITATED CONDITIONS

The structural characteristics of the aggregates can also be classified using fluorescent dye 1-anilinonaphthalene-8-sulfonate (ANS). Fluorescence spectroscopy is an attractive method for studies, due to sensitivity, ease of use, and flexibility. ANS is non-fluorescent in water (polar environment) but is highly fluorescent in hydrophobic environments. ANS binding with proteins is associated with two simultaneous events i.e. increase in fluorescence intensity and a blue shift of ANS fluorescence.

ANS is sulfonated naphthalene with Aniline group (figure 2.3). The naphthalene backbone and the aniline group are hydrophobic, but sulfonate group has negative charge. Amide at the aniline ring can provide electrons for hydrogen bond formation with a protein. Using sulfonate group ANS can interact with positively charged amino acids.

ANS is widely used to measure exposed hydrophobic patches on proteins, and presence of exposed hydrophobic patches is a common feature of highly toxic soluble aggregates.
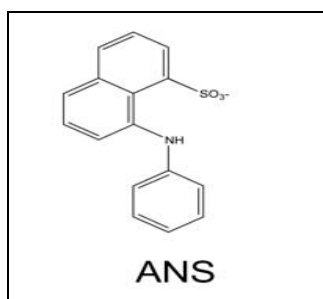

Figure 2.3: Structure of ANS, 1-anilinonaphthalene-8-sulfonate

Aliquots of protein solutions after incubation for at 37 degree Celsius to form amyloids were taken and diluted to give a 50 μM concentration in 200 mM ANS. Spectra max was used to record fluorescence spectra between 400 and 600 nm upon excitation of the sample at 380 nm.

2.5. PROBING THE ACCESSIBILITY OF TRYPTOPHAN IN SOLUBLE PROTEIN VS AMYLOID AGGREGATES

HEWL has six tryptophan (Trp) residues, Trp 28, 62, 63, 108, 111, 123. Among these residues, Trp 62, Trp 63 and Trp 123 are solvent accessible. The fluorescence emission of tryptophan undergoes a blue shift when the polarity of its environment decreases. Intrinsic tryptophan fluorescence can be a useful probe for the characterization of aggregates formed.

The intrinsic fluorescence spectra of Trp were measured on fluorescence spectrophotometer (spectra max M5e) with a cuvette of 1cm path length at room temperature. The concentration of HEWL protein samples were initially determined by using the absorbance value at 280nm. The molar extinction coefficient of lysozyme is 2.56 M^{-1} $CM^{-1.}$ For Trp emission spectra, the excitation wavelength was at 295 nm and the emission spectra were recorded in the wavelength range of 300 – 400 nm.

Acrylamide Quenching:

Fluorescence quenching is a process which decreases the intensity of the fluorescence emission. The accessibility of Trp group on monomeric lysozyme and amyloidogenic form can be measured by use of quenchers. Quenching by acrylamide occurs by collisional mechanism. Here the quencher, acrylamide deactivates the excited state and since collisional or dynamic quenching depopulates the excited state without allowing fluorescence emission, the fluorescence intensity decreases.

Acrylamide quenching of Trp fluorescence was carried out by measurement of fluorescence intensity before and after addition of small aliquots of freshly prepared acrylamide solution (x M). The assay was performed on both agitated, non-agitated and the monomeric lysozyme. The Trp fluorescence intensity was recoded before and after adding the acrylamide quencher. The mixture was incubated for 5 minutes in the dark. The emission spectrum was scanned from 300-400 nm by setting the excitation wavelength to 295 nm.

2.6. SELF-SEEDING OF SOLUBLE LYSOZYME BY PREFORMED FIBRILS

Amyloids exhibit a key phenomenon known as seeding i.e. the rate of formation of fibrils by amyloidogenic protein increases by the addition of preformed fibrils [12]. The seeds act as a starting material or template for the assembly and growth of amyloid fibers. This also acts as a basis for the spread of amyloid deposits in tissues and from one organ to another in case of systemic amyloidosis. The growth of amyloid shows sigmoidal growth curve with three phases:

a) Initial lag phase, during which oligomer protein "seed" or nucleus is formed

b) In the log phase also called as exponential phase or polymerization phase, seeds recruit the monomeric protein molecules in exponential manner.

c) In the last phase called the stationary phase, amyloid is formed completely with no further increase in fibrillization process.
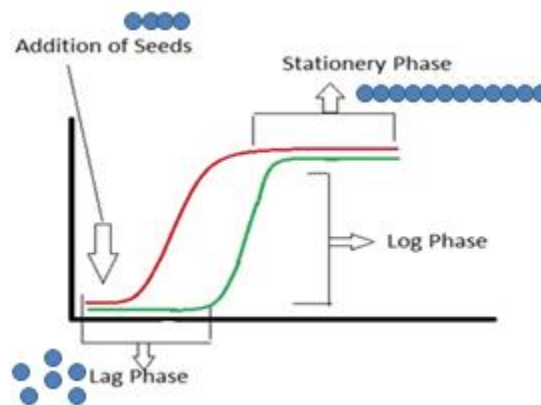
Figure 2.4: Growth of amyloid fibrils shows sigmoidal growth curve

The molecular organization of amyloid fibrils is generally same since all the amyloid fibrils contains monomers packed in cross-beta fashion. Nevertheless fibril formation is specific, with subtle differences in the interaction between the beta strands making seeding specific. Seeding affects the kinetics by decreasing the lag phase and thus over all time to form the amyloid.

Sonication: High frequency sound waves are generated for the disassembly of large amyloid polymers to small oligomer seeds with suitable for growth of amyloid. It is the ultrasound (amplitude 20%) that is applied to the amyloid samples. Using 70% ethanol the probe was first cleaned and then the microcentrifuge tube containing 100 µl of amyloid sample was sonicated three times for 10 seconds each on ice. Since some heat

may generate during the sonication process, it was preferred to wait for 5 seconds between each cycle.

The high frequency is generated electronically and the mechanical energy is transmitted to the sample via a metal probe that oscillates with high frequency thus breaking the amyloid fibrils into smaller seeds with suitable ends for the growth of amyloid.

Seeding kinetics: To outline the seeding conditions, 5 µl of sonicated solution of preformed HEWL fibrils was added to 95 µl of fresh solution of the protein made in glycine – HCl buffer, pH 2.0, with 5 µl of ThT in 96-well plate to observe the kinetics with increase in thioflavin T fluorescence. Seeding kinetics was observed using spectra max fluorimeter. The experiment was set for 99 hours to record the ThT emission intensity with excitation at 450 nm and emission at 485 nm at an interval of 3 minutes.

Preformed HEWL amyloid
solution, at 37 °C, pH 2.0

Sonication

Bigger aggregates
disassemble into smaller
oligomeric "seeds"

Addition of 5 % seed to
fresh solution of lysozyme in
glycine HCl buffer pH 2.0

Seeding kinetics recoded for
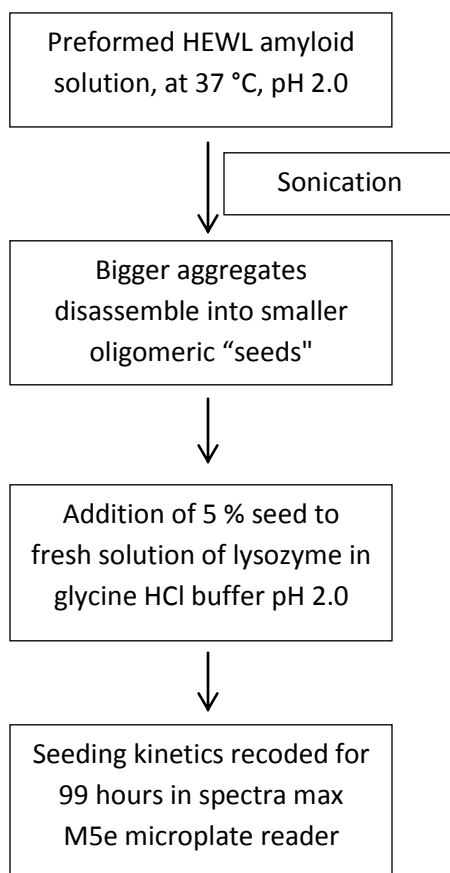99 hours in spectra max
M5e microplate reader

Figure 2.5: Procedure for studying seeding kinetics of HEWL

2.7. STABILITY OF LYSOZYME AMYLOID TOWARDS DETERGENT

Soluble proteins generally dissolve in detergents like SDS and N-Lauroylsarcosine sodium salt whereas the amyloid like aggregates can survive these conditions. Stability against detergents is one of the key features of amyloid where the bulky aggregates disassemble on treatment with detergents into smaller aggregates, yet partially stable. For assessing the sarkosyl stability of the lysozyme amyloid aggregates at room temperature a method called Semi Denaturing Detergent Agarose Gel Electrophoresis (SDD-AGE) was used. This method was described by Kryndushkin et al. in the year 2003 [39].

Since the aggregates are bigger in size they cannot be analyzed in polyacrylamide gel which has small pores. The pore size is not sufficient for the passage and resolution of amyloid like aggregates thus agarose gel was used for running the large protein polymers. Kryndushkin DS, et al., (2003) suggested the separation of yeast prion [PSI+] in agarose gel followed by western blotting on nitrocellulose membrane to observe the size of SDS-resistant amyloid aggregates of yeast prion [PSI+] [39].

SDD-AGE is short form of Semi Denaturing Detergent Agarose Gel Electrophoresis. This method enables the characterization of large protein polymers which are stable in SDS or Sarkosyl at room temperature. Amyloid fibrils are insoluble and thus difficult to study. However they can be resolved based on their size and detergent insolubility using the method SDD-AGE. The conformational variants can be characterized for their difference in stability against detergents and size using this technique. The process involves the following four steps:

1. Preparation of the agarose gel
2. Preparation of HEWL samples
3. Agarose gel electrophoresis
4. Transfer to Polyvinylidene difluoride (PVDF) membrane
5. Detection of protein on PVDF membrane

Buffers and reagents: Buffer for making agarose gel (1.5%): Tris = 20mM, Glycine = 200mM, Agarose = 1.5%, SDS = 0.1%; Sample buffer (4x) without SDS and DTT: Tris

= 240mM, Bromophenol blue = 0.2%, Glycerol = 2.0%; Electrophoresis running buffer: Tris = 20mM, Glycine = 200mM, SDS = 0.1%; Transfer buffer: Tris = 20mM, Glycine = 200mM, SDS = 0.1 %, Methanol = 1.5%; Staining solution: coomassie brilliant blue R-250 = 0.4 g, methanol = 30%, acetic acid = 10%; Destaining solution: Methanol = 30%, acetic acid = 10%.

Step 1: Preparation of the agarose gel

a) 1.5% agarose gel was prepared in tris-glycine buffer. The weighed amount of agarose was completely dissolved using microwave.

b) After agarose melted 0.1% SDS was added drop wise from 10% stock with gentle swirling to avoid bubble formation.

c) Agarose solution was then poured into the casting tray enough for submerging the comb teeth.

d) After the gel was set, comb was removed and the gel was placed in the gel tank containing the electrophoresis buffer with 0.1% SDS.

Step 2: Preparation of HWEL samples

a) To an aliquote of HEWL amyloid fibril, sarcosyl solution was added from 10% stock such that the final concentration of sarcosyl becomes 2 %.

b) The mixture was incubated for 10 minutes to check for the stability of amyloid fibrils against the mild detergent sarcosyl.

Step 3: Agarose gel electrophoresis

a) From the 4X stock of sample buffer, aliquots were added to the samples to generate mixture containing 1X sample duffer.

b) Samples with 1X sample buffer were incubated at room temperature for 5 minutes and were then loaded in gel.

c) The gel was allowed to run at 125 volts for half an hour.

Step 4: Transfer to PVDF membrane

a) A piece of nitrocellulose membrane was cut to the same dimensions as the agarose gel.

b) Two pieces of blotting paper were also cut in same dimensions as gel

c) The nitrocellulose membrane was then allowed to soak in distilled water. It should be wetted carefully laying it on the surface of water and allowing the nitrocellulose membrane to wet from the bottom by capillary action.

d) After wetting it in distilled water the membrane was submerged in methanol for 1 minute which acts as activator.

e) In a plastic container, both the blotting paper and the nitrocellulose membrane were then soaked in transfer buffer.

f) The agarose gel was trimmed and oriented by making a cut in the lower right hand corner.

g) Then each module was assembled in the following order starting from the bottom electrode plate (the cathode): First a black foam pad was placed on the bottom of electrode plate, then a thick absorbent/blotting paper, thoroughly soaked in transfer buffer, a wet nitrocellulose membrane, the agarose gel, a thick absorbent paper, a single folded mesh and then the upper electrode (the anode).

h) While assembling the stack, bubbles were carefully removed by lifting the edges of the membrane.

i) The electrodes were then connected and transfer was allowed to proceed for a minimum of 2.5 hours at 100 volts, inside the refrigerator at 4 °C.

Step 5: Detection of protein on PVDF membrane

After transfer the membrane was stained with Coommassie R-250 for 5 minutes.

Membrane was destained overnight with destaining solution and the image was captured using gel doc (G:box, syngene).

2.8. STABILITY OF HEWL AMYLOIDS AT PHYSIOLOGICAL pH

Stability of lysozyme amyloid formed under agitated vs non-agitated condition at pH 2.0 was checked under physiological pH of 7.4. Human lysozyme variants are known to form amyloid *in vivo* leading to non-neuropathic amyloidosis. HEWL is known to form amyloid *in vitro* at low pH of 2.0. Thus to check if the HEWL amyloid formed *in vitro* is also stable at physiological pH the following assay was performed.

The HEWL is usually fibrillized in glycine – HCl buffer of pH 2.0, 0.5 M. The pH of the HEWL amyloid fibril solution was brought to pH 7.4 by mixing it with excess of Tris–HCl buffer of pH 7.5, 0.6M. The details of the assay are tabulated below:

Table 2.1: Preparation of sample mixtures for pH stability assay

Samples	Lysozyme amyloid	Glycine HCl buffer pH 2.0, 0.5 M	Tris HCl buffer pH 7.5, 0.6M	Glycine HCl buffer pH 2.0, 0.6 M	Total
Static amyloid	20 µl		80 µl		100 µl
Agitated amyloid	20 µl		80 µl		100 µl
Blank 1		20 µl	80 µl		100 µl
Blank 2		20 µl		80 µl	100 µl
Control for Static amyloid	20 µl			80 µl	100 µl
Control for Agitated amyloid	20 µl			80 µl	100 µl

2.9. STABILITY OF HEWL AMYLOIDS AGAINST DENATURANTS LIKE UREA

To further investigate the stability of agitated vs non agitated fibrils, urea induced dissociation assay was performed. Urea is a nonionic chaotropic agent that denatures proteins by disrupting the hydrophobic interaction. Denaturants like urea weakens the hydrophobic and hydrogen-bonding interactions, thus disrupting aggregation and shifting the equilibrium towards monomers.

Urea was purchased from Sigma Aldrich. 5M stock urea was prepared in 0.5M glycine –HCl buffer at pH 2.0. Here we employed ThT fluorescence as a measure to study the extent of dissociation in presence of urea. After equilibrating the amyloid fibrils in increasing concentration of urea for 30 mins, Thioflavin T was added and fluorescence end points were recorded using 96-well plate. The data was then analyzed by plotting the fluorescence endpoints against increasing concentrations of urea.

2.10. ENZYME ACTIVITY ASSAY OF SOLUBLE HEWL AND ITS AMYLOID FORMS

10 µl aliquots each of soluble lysozyme dissolved in assay buffer of sodium phosphate (100mM, pH 7.4), soluble lysozyme dissolved in fibrillization buffer, and the amyloid forms were placed in alternate individual wells of 96-well microplate. A suspension of *Micrococcus lysodeikticus* cells (3 mg) was made in 10 ml of sodium phosphate assay buffer shortly before the assay. 190 µl of suspension was added to each well containing the lysozyme samples. Cell lysis was monitored at an absorbance of 595 nm with intermittent shaking and readings were recorded for a time span of 60 minutes at an interval of 30 seconds. The results were then plotted against time in X-axis.

CHAPTER III
RESULTS

3.1. CONFIRMATORY ASSAYS FOR HEWL AMYLOID AGGREGATES

3.1.1. Thioflavin – T (ThT) binding assay

ThT emission fluorescence intensity was measured after incubating the protein HEWL for 7 days at 37 °C, pH 2.0 glycine HCl buffer (Excitation wavelength = 450 nm ; Emission wavelength = 485 nm).The samples were incubated with or without agitation in the same buffer for the amyloid growth. Increase in ThT fluorescence intensity and shift in excitation and emission maxima of ThT fluorescence were observed similar to as expected for amyloid aggregates (**Table 3.1; Figures 3.1 & 3.2**). The higher ThT fluorescence intensity observed for aggregates formed under agitated incubation could be due to increase in the number of binding sites for ThT and possibly indicate different structural organization in these aggregates.

Table 3.1: Thioflavin T fluorescence intensity

Sample	ThT Fluorescence intensity		
	Protein at 4 °C	Protein at 37 °C (non-agitated)	Protein at 37 °C (agitated)
Blank	107.9	126.9	238.0
HEWL	272.2	2823.1	4603.7

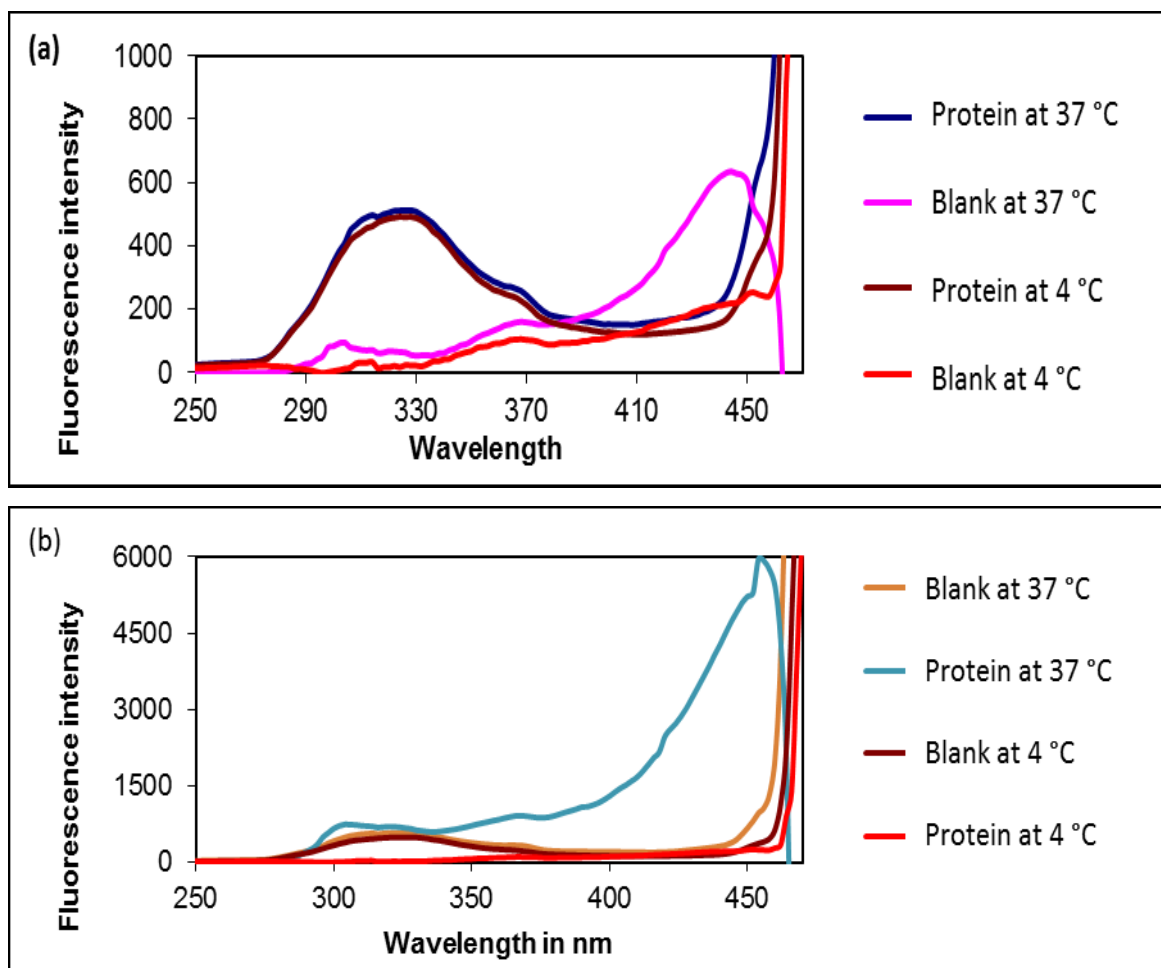Figure 3.1: Excitation spectrum of HEWL amyloids (a) Static (b) agitated (Emission wavelength = 485 nm, Excitation scanned from 250 – 470 nm). The respective blanks were subtracted before plotting the data.
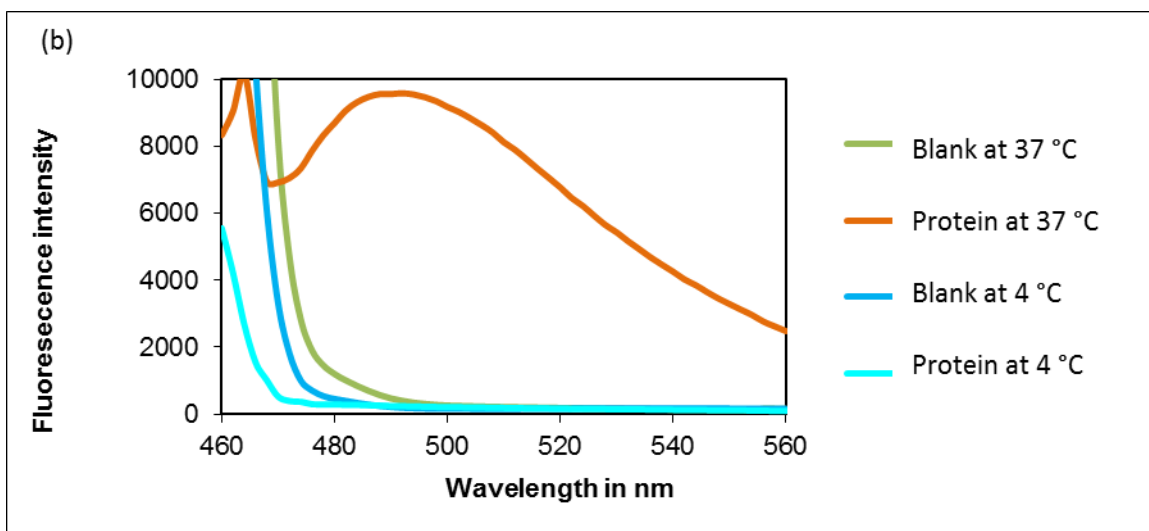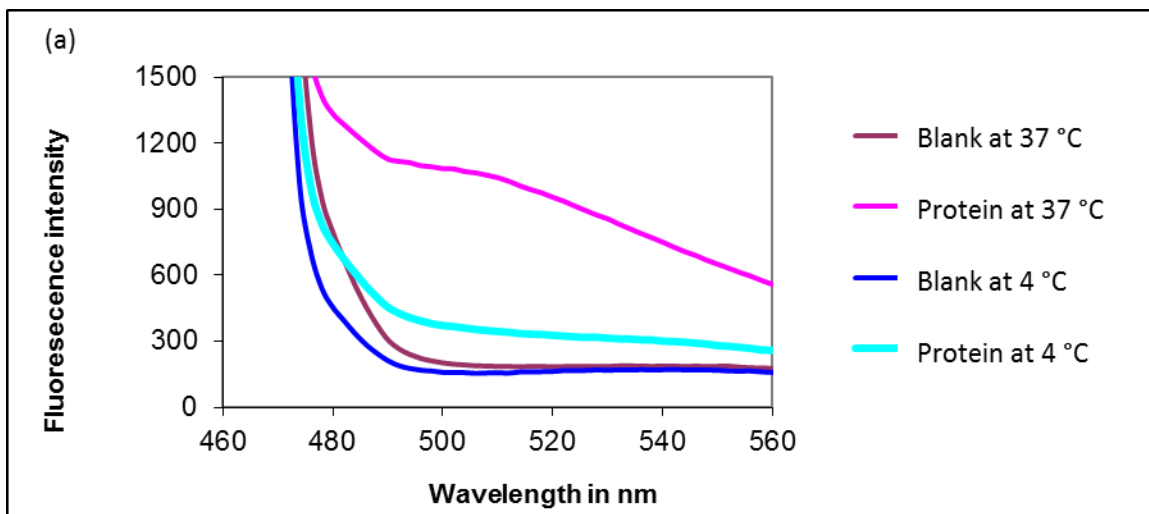
Figure 3.2: Emission spectrum of HEWL amyloids (a) Static (b) agitated (Excitation wavelength = 450 nm, emission spectra scanned from 460 – 560 nm). The respective blanks were subtracted before plotting the data.

3.1.2. Congo red (CR) binding assay

Absorption spectrum of Congo red was recorded from 300 – 700 nm after incubating the protein-Congo red mixture for 30 minutes. A shift in the absorption peak from 490 nm to 540 nm in the mixture of lysozyme amyloid and Congo red strongly suggests presence of amyloid like structure in the aggregates (**Figure 3.3**).
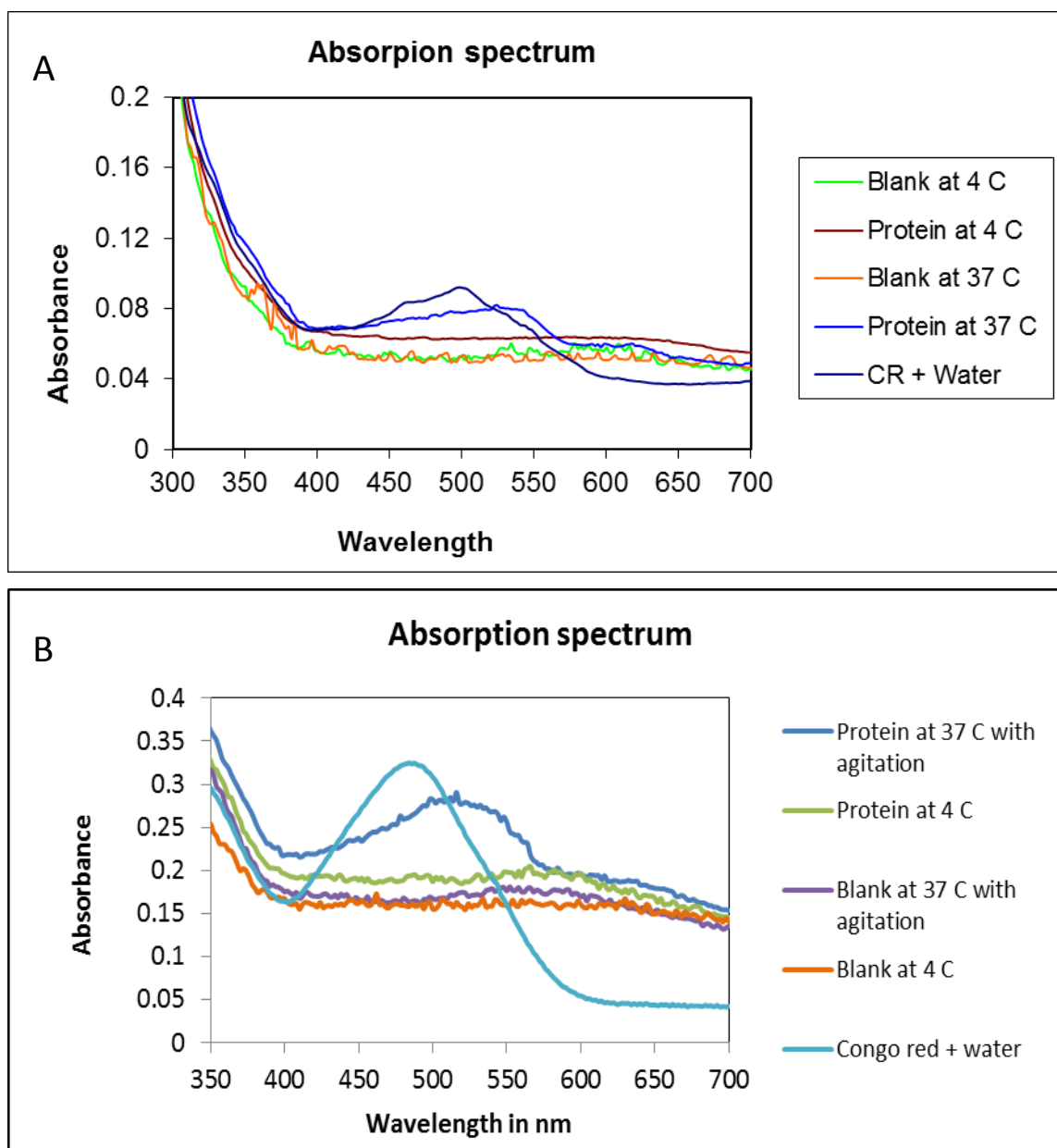
Figure 3.3: Absorption spectrum of Congo red with HEWL aggregates (a) Static (b) Agitated

3.2 ANALYSIS OF TURBIDITY BY LIGHT SCATTERING

When amyloid aggregates are formed, the turbidity of the solution increases due to accumulation of aggregate particles. Using fluorescence light scattering, we checked if the HEWL samples exhibited turbidity. The samples were excited at 450nm and emission was measured at same wavelength as an estimate of turbidity. Results showed higher scattering in case of HEWL incubated in the fibrillization buffer for 7 days at 37 °C, pH 2.0 thereby indicating the formation of higher size entity which is consistent with amyloid formation **(Table 3.2)**. Possibly, the difference in the extent of light scattering of the static vs agitated samples could be a reflection of differences between two amyloids with regards to particle size or number of aggregates

Table 3.2: Turbidity measurement of soluble and amyloid forms of HEWL

Samples	Fluorescence Emission intensity (A.U)
Buffer	4976.9
Soluble protein	5898.0
Non-agitated amyloid	11828.5
Agitated amyloid	7363.0

3.3. PROBING THE ACCESSIBILITY OF TRYPTOPHAN IN SOLUBLE PROTEIN vs AMYLOID AGGREGATES

Previously it has been reported that fluorescence of Trp residues in amyloidogenic K peptide of HEWL can be quenched by 62% in soluble form and only 41% after fibrillization [39]. K-peptide is a small peptide of 8 amino acid residues. Compared to the K-peptide, the fluorescence of Trp residues in full length HEWL protein could be quenched by 28 % in soluble form and only 23 % in fibrillized form. The peptide with random coil structure may have tryptophan more accessible whereas the full length protein has tryptophan already inaccessible thus it is showing only marginal differences **(Table 3.3 & Figure 3.4)**. The results indicate that HEWL amyloids require more acrylamide for quenching of Trp fluorescence suggesting relatively buried Trp residues. There was, however, no perceivable difference between the static vs agitated amyloid aggregates with regards to the burial of tryptophan residues.

Table 3.3: Tryptophan fluorescence of HEWL with acrylamide (0.05 M) quencher

	I_{max} before quenching	I_{max} after quenching	Percentage quenching (%)
Soluble Protein	3062	2191	28.45
Static amyloid	3029	2316	23.54
Agitated amyloid	2702	2073	23.28
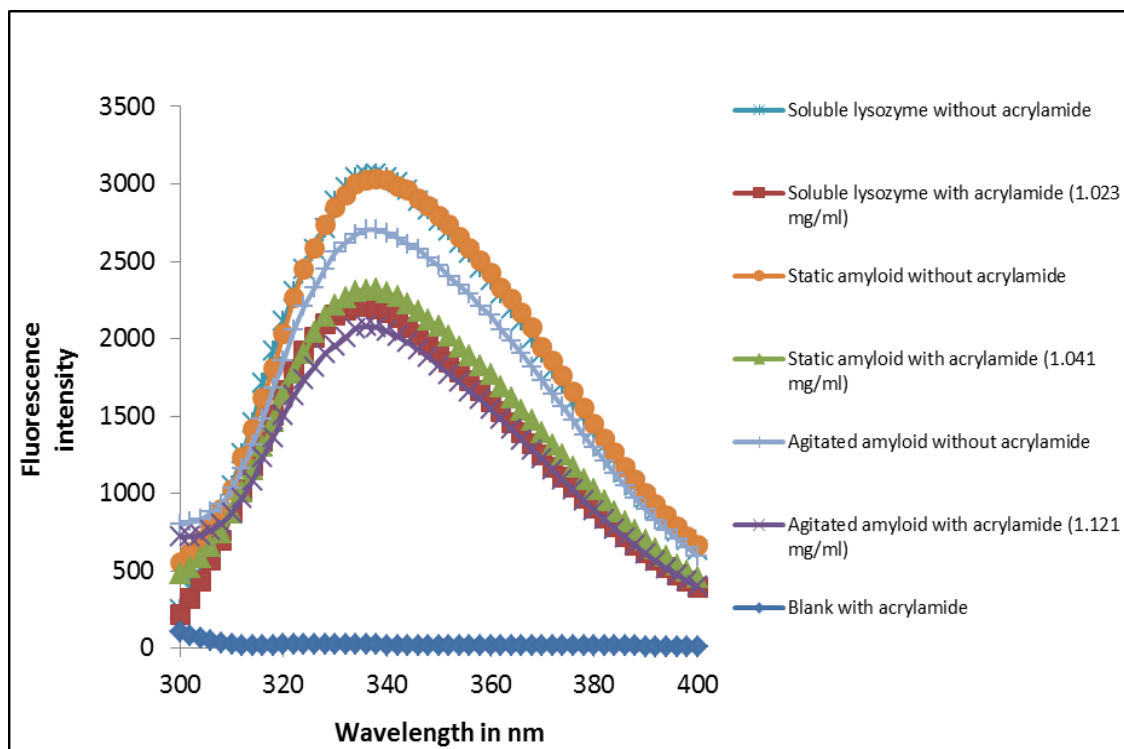
Figure 3.4: Trp Fluorescence emission spectra with quencher, 0.05M acrylamide.

3.4. ANALYSIS OF HYDROPHOBIC REGION BY ANS BINDING OF HEWL AMYLOID FORMED UNDER STATIC VS AGITATED CONDITIONS

The fibrillization of HEWL was carried out at acidic pH and elevated temperatures. With decrease in pH partial unfolding of a protein may result leading to exposure of few hydrophobic regions. ANS, which shows high affinity for hydrophobic patches of protein, was found to bind HEWL at pH 2.0 as evident by increased ANS fluorescence intensity and blue shift in λmax to ~488 nm from 510 nm **(Figure 3.5 & Table 3.4)**. The amyloid forms of HEWL were found to be more amenable to ANS binding possibly indicating increase in hydrophobic patches due to conformation change of the protein under amyloid forming condition i.e. pH 2.0 and high temperature, 37°C. Static amyloid exhibited a little higher ANS binding relative to the agitated amyloid, possibly indicating conformational difference between the two amyloids **(Table 3.4)**.
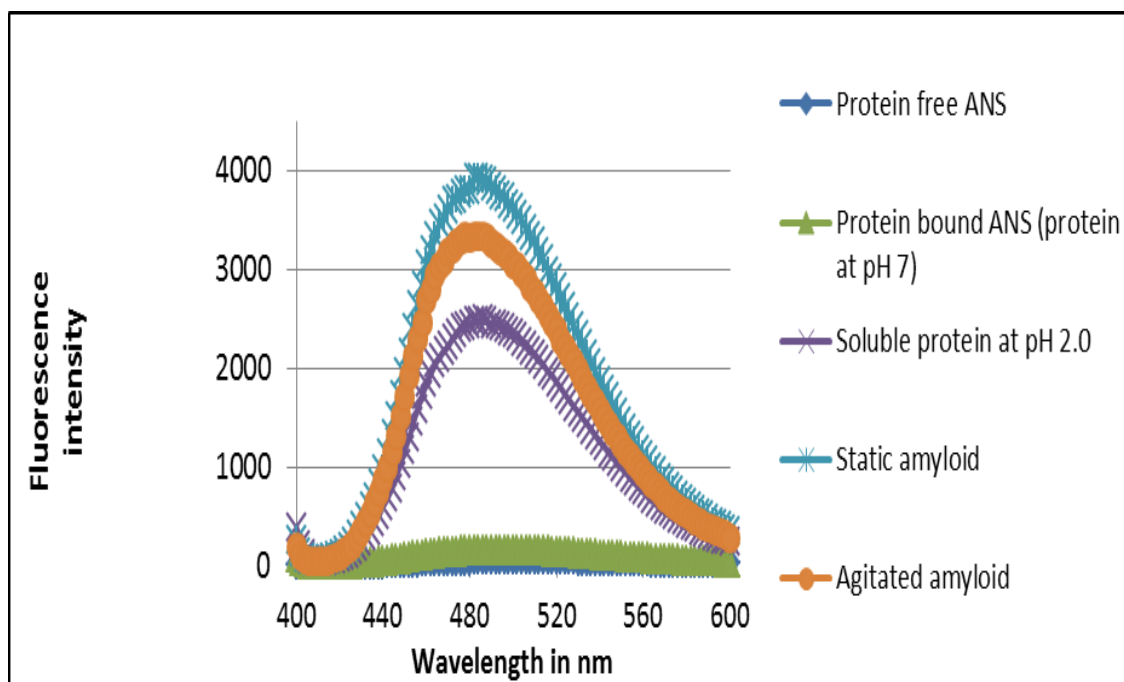
Figure 3.5: Binding of ANS to HEWL amyloids assayed by its extrinsic fluorescence (Excitation: 350 nm and Emission: 400-600 nm)

Table 3.4: ANS fluorescene upon binding to HEWL amyloid aggregates

Sample	ANS Fluorescence Emission	
	I_{max} (A.U)	λ_{max}
Only ANS	58.14	510 nm
ANS + Soluble protein pH 7.0	156.22	488 nm
ANS + Soluble protein pH 2.0	2492.39	486 nm
Agitated amyloid	3344.86	482 nm
Static amyloid	3931.07	484 nm

3.5. SELF-SEEDING OF SOLUBLE LYSOZYME BY PRE-FORMED FIBRILS

As amyloid aggregates have well organized structure, they show striking ability of seeding their un-aggregated counterpart native proteins, thereby converting it also into the amyloid form. This process of seeding is highly specific process and depends on the conformational compatibility of the amyloid seed and the un-aggregated protein. It is known that prion variants are result of amyloid conformational variants, which either do not cross-seed or cross-seed each other highly inefficiently. As we succeeded in aggregating HEWL under two conditions, we asked if these amyloids have same or different conformations by examining whether they can cross-seed each other. First, we checked whether these aggregates show self-seeding of the monomeric protein under the conditions in which they were previously aggregated. For this, we examined the:

1. Self-seeding of HEWL incubated under static condition by seed samples pre-aggregated under static conditions.
2. Self-seeding of HEWL incubated under agitated condition by seed pre-aggregated under agitated conditions.

Next, we checked the conformational cross-seeding ability of these two HEWL amyloids by examining:

1. Cross-seeding of HEWL incubated under agitated condition by seed pre-aggregated under static conditions
2. Cross-seeding of HEWL incubated under static condition by seed samples pre-aggregated under agitated conditions

The experimental design to check the above mentioned seeding abilities and the outcome has been schematically summarized in **Figure 3.6.**

```
┌─────────────────────────────────┐          ┌─────────────────────────────────┐
│ HEWL amyloid formed at 37 °C,   │          │ HEWL amyloid formed at 37 °C,   │
│                                 │          │                                 │
│ pH 2.0, WITHOUT agitation       │          │ pH 2.0, WITH agitation          │
└─────────────────────────────────┘          └─────────────────────────────────┘
            │     ┌──────────────┐                       │     ┌──────────────┐
            │     │  Sonication  │                       │     │  Sonication  │
            ▼     └──────────────┘                       ▼     └──────────────┘
┌─────────────────────────────────┐          ┌─────────────────────────────────┐
│     Amyloid Seeds generated     │          │     Amyloid Seeds generated     │
└─────────────────────────────────┘          └─────────────────────────────────┘
```

Self-seeding │   Conformational   Self-seeding │   Conformational
             ▼   cross-seeding │   ▼   cross-seeding │
                                      ▼   ▼

```
┌──────────────────┐  ┌──────────────────┐   ┌──────────────────┐  ┌──────────────────┐
│ Seeding of HEWL  │  │ Seeding of HEWL  │   │ Seeding of HEWL  │  │ Seeding of HEWL  │
│ WITHOUT agitation│  │ WITH agitation   │   │ WITH agitation   │  │ WITH OUT agitation│
└──────────────────┘  └──────────────────┘   └──────────────────┘  └──────────────────┘
         │                     │                      │                      │
         ▼                     ▼                      ▼                      ▼
┌──────────────────┐  ┌──────────────────┐   ┌──────────────────┐  ┌──────────────────┐
│ Result:          │  │ Result:          │   │ Result:          │  │ Result:          │
│ Self-seeding     │  │ No cross-seeding │   │ Self-seeding     │  │ No cross-seeding │
│ observed         │  │ observed         │   │ observed         │  │ observed         │
│ (Figure 3.7)     │  │ (Figure 3.9)     │   │ (Figure 3.8)     │  │ (Figure 3.10)    │
└──────────────────┘  └──────────────────┘   └──────────────────┘  └──────────────────┘
```
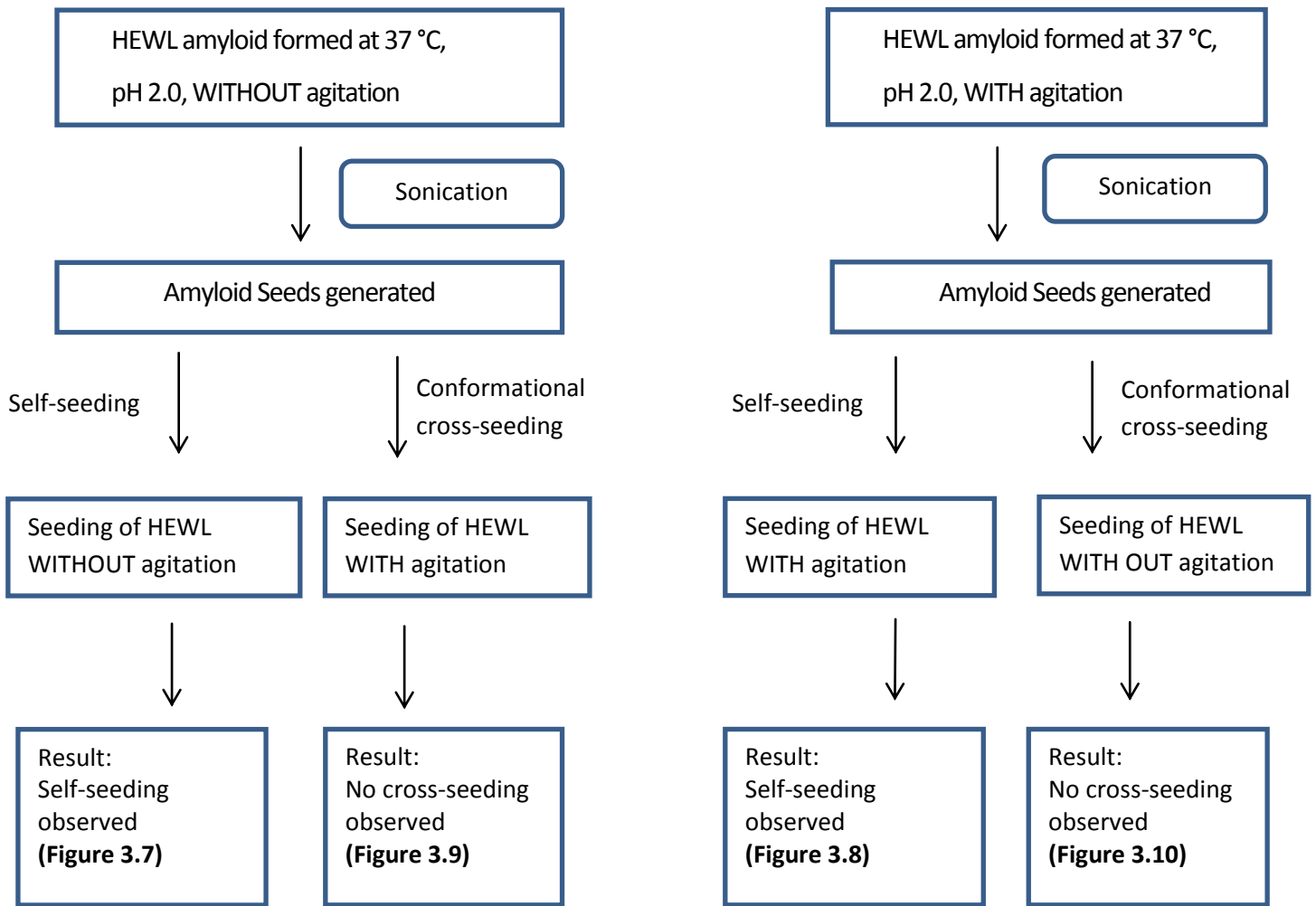
Figure 3.6: Schematic assay of ability of self-seeding and conformational cross-seeding by HEWL amyloid aggregates and results obtained.
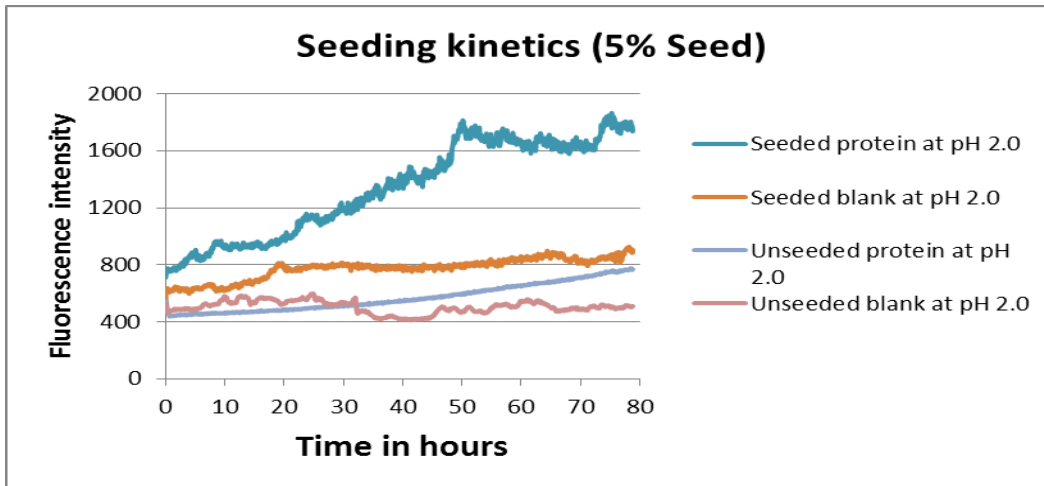
Figure 3.7: Self-Seeding kinetics of static HEWL with 5% static seeds, self-seeding. The protein entered log phase immediately with reduced lag time. The amyloid was formed in 49 hours in seeded conditions whereas it takes 168 hours to form amyloid without seeding.
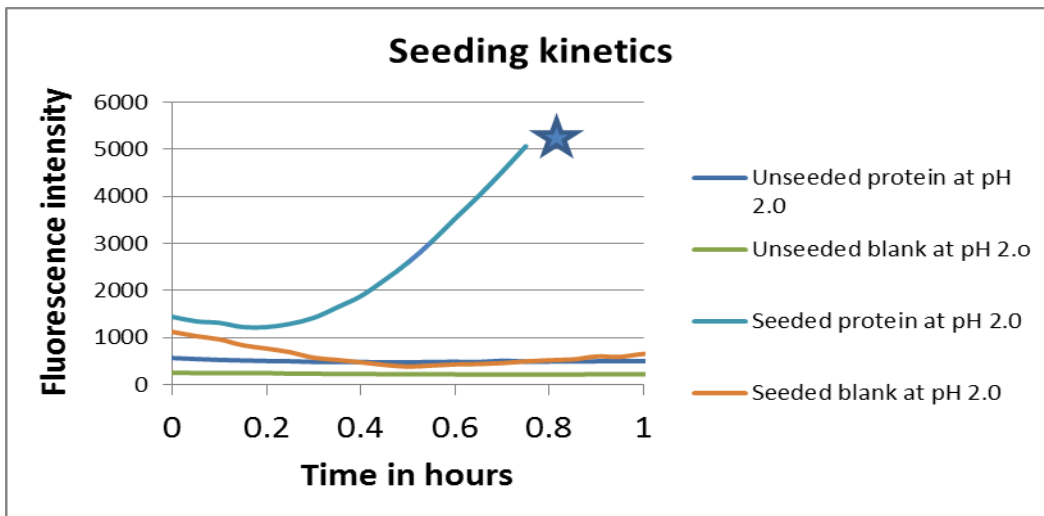

Figure 3.8: Seeding kinetics of agitated samples HEWL with agitated seeds (self-seeding).

★Detectors saturation point reached: Shows high fluorescence intensity of amyloid. A strong hint of seeding was observed in this case with very high and increased fluorescence intensity in case of seeded protein within an hour. The results from self-seeding of HEWL confirm the amyloid formation as seen in other amyloids.
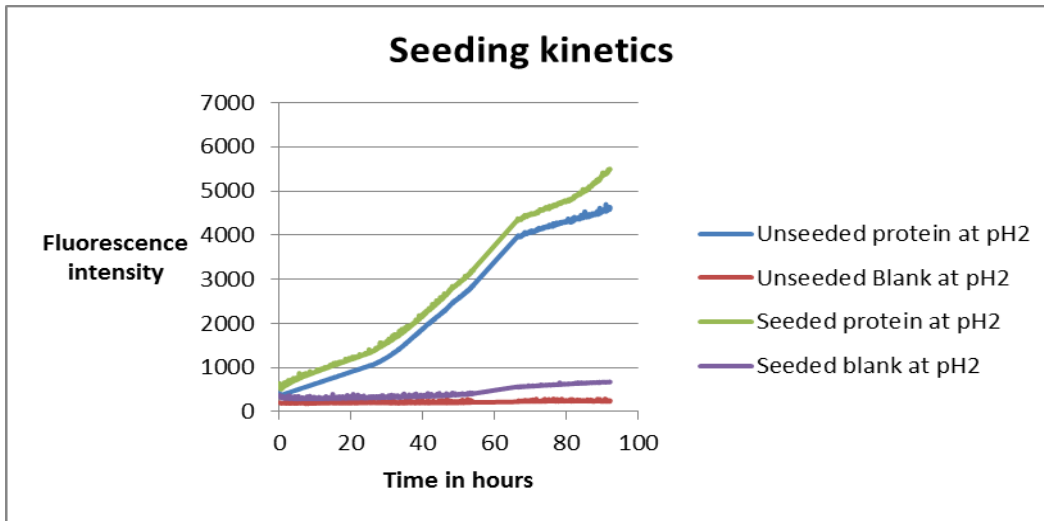
Figure 3.9: Conformational cross-seeding kinetics of agitated HEWL with static seeds. The agitation reduces the time required for the amyloid formation. Seeds from static samples could not show any effective seeding even with 5% seed, suggesting conformational variation between the two amyloids.
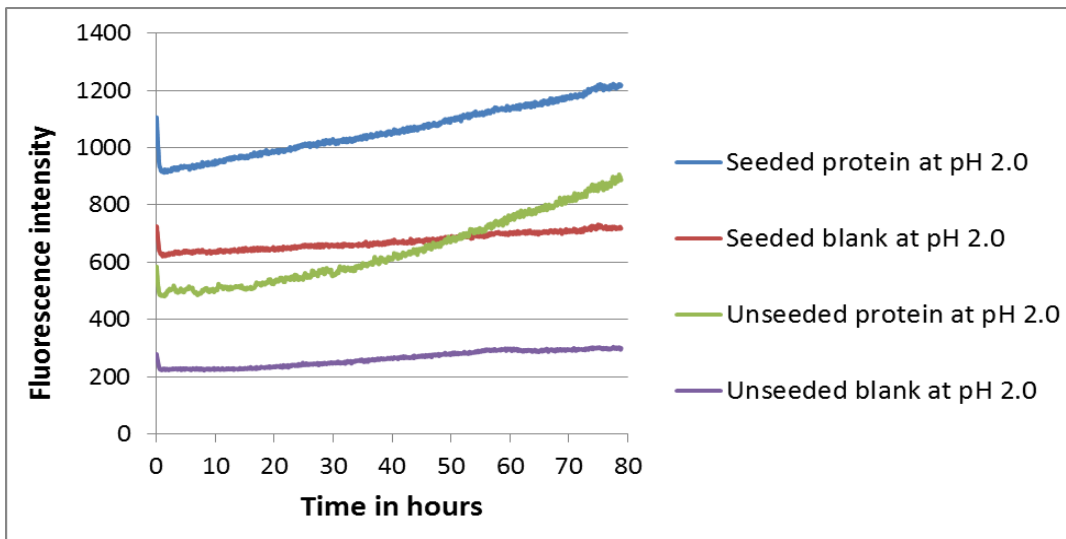

Figure 3.10: Conformational cross-seeding kinetics of static HEWL samples with agitated seeds

Apparently, the seeds from agitated samples could not seed the protein under static conditions further suggesting conformational variation between the two amyloids. Very slow growth of amyloid was observed both in case of seeded and unseeded samples under static conditions.

3.6. ANALYSIS OF RELATIVE STABILITY OF STATIC VS AGITATED HEWL AMYLOID AGGREGATES

If the HEWL amyloid aggregates formed under different conditions (here agitated & static) represent variant conformations, they may be expected to have different stabilities. To examine this, we assayed the relative stabilities of the static versus agitated condition made aggregates against the detergent sarkosyl, pH change and the denaturant urea. Indeed we found that, while both aggregates are stable to complete dis-aggregation by Sarkosyl, they also exhibit different range of sizes of oligomers/polymers **(Figure 3.11)**. The HEWL aggregates formed at static incubation showed higher size sarkosyl-resistant polymers as compared with the agitated aggregates.
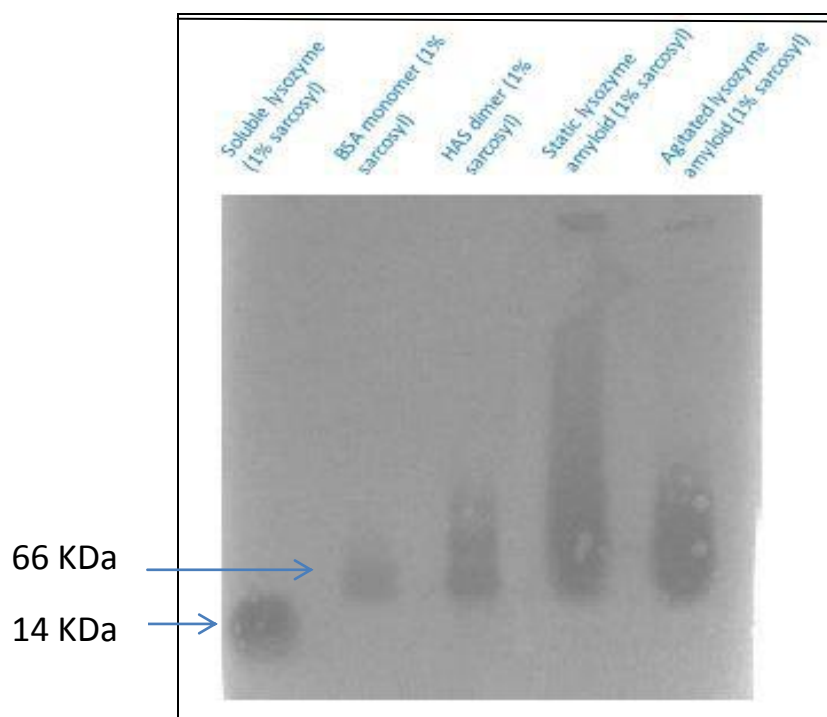

Figure 3.11: Analysis of sarkosyl resistance of static and agitated HEWL amyloid aggregates by SDD-AGE. For this the samples were incubated with sample buffer containing 1% sarkosyl at room temperature for 10 minutes and then electrophoresed on 1.5% agarose followed by electroblotting on PVDF membrane. Finally, protein was visualized by Coommassie staining.

Using the relative mobility **(Table 3.5)** of three proteins of known molecular weights (Lysozyme, BSA & HSA homo-dimer), a calibration curve **(Figure 3.12)** was generated which helped in the estimation of molecular weight of the sarkosyl-resistant polymers from the HEWL amyloid aggregate formed by agitation or under static incubation. From this, the molecular weight of the biggest sarkosyl-resistant polymer in static lysozyme amyloid was estimated to be~ 4671 KDa which would contain over 330 monomers of HEWL. In comparison, the molecular weight of the biggest sarkosyl-resistant polymer in agitated lysozyme amyloid was estimated to be 864.56 KDa (~ 60 monomers) suggesting that either the agitated amyloid aggregates are smaller in size in general or they are more fragile susceptible to sarkosyl dis-aggregation relative to the static amyloid. This strongly suggests that the two forms of the HEWL amyloid are indeed amyloid variants. Similar detergent-resistant size differences have been previously observed for yeast [PSI+] prion where the strong variant of [PSI+] shows shorter aggregates of Sup35 amyloid relative to the weak variant of [PSI+] [40].

Table 3.5: Relative mobility of protein samples and HEWL amyloids on SDD-AGE

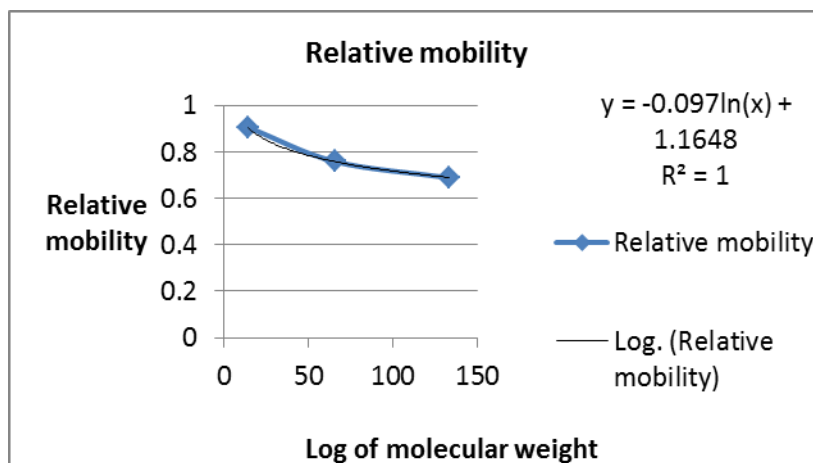| Protein sample	Distance moved in cm [X]	Gel front in cm [Y]	Relative mobility [X/Y]
Lysozyme (14 Kda)	5.0	5.5	0.909
BSA (66KDa)	4.2	5.5	0.7636
HSA dimer (134KDa)	3.8	5.5	0.69
Lysozyme amyloid (Static)	1.9	5.5	0.3454
Lysozyme amyloid (agitated)	2.8	5.5	0.509

Figure 3.12:

We further tested the stabilities of the two types of amyloid aggregates against change in pH by measuring ThT fluorescence emission and excitation intensities **(Figure 3.13)**. First the aggregates pre-made in the fibrillization buffer pH 2.0 were shifted to pH 7.0 and allowed to equilibrate. Subsequently ThT emission and excitation intensities at 485nm and 450 nm were recorded as described in the methods. While the aggregates formed by agitation showed partial dis-aggregation by this pH change, the aggregates made under static conditions were remarkably stable to this pH change **(Figure 3.13 & Figure 3.14)**. This observation further supports variant amyloid conformation in the two types of aggregates.
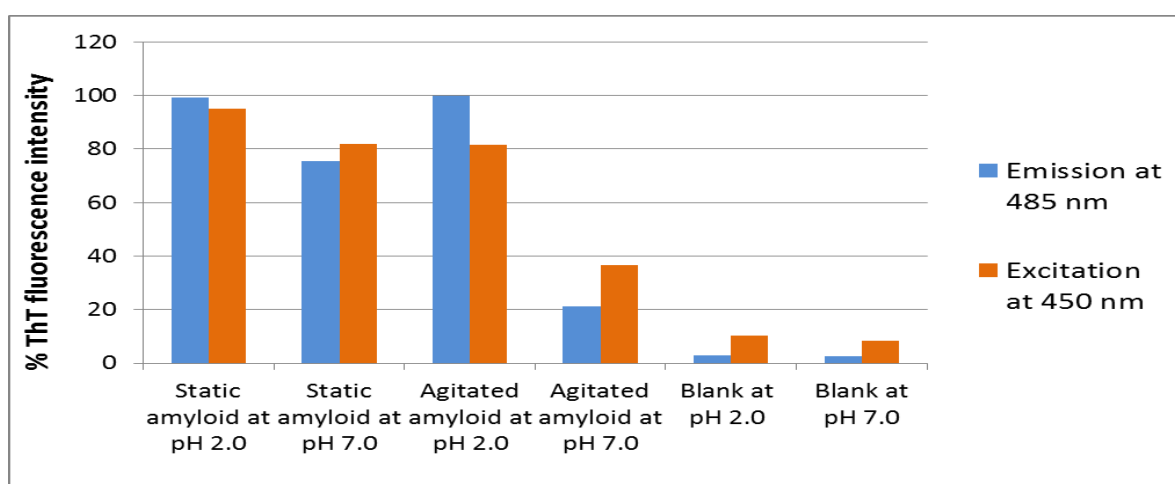

Figure 3.13: Comparison of HEWL amyloids stability at pH 2.0 *vs* pH 7.0
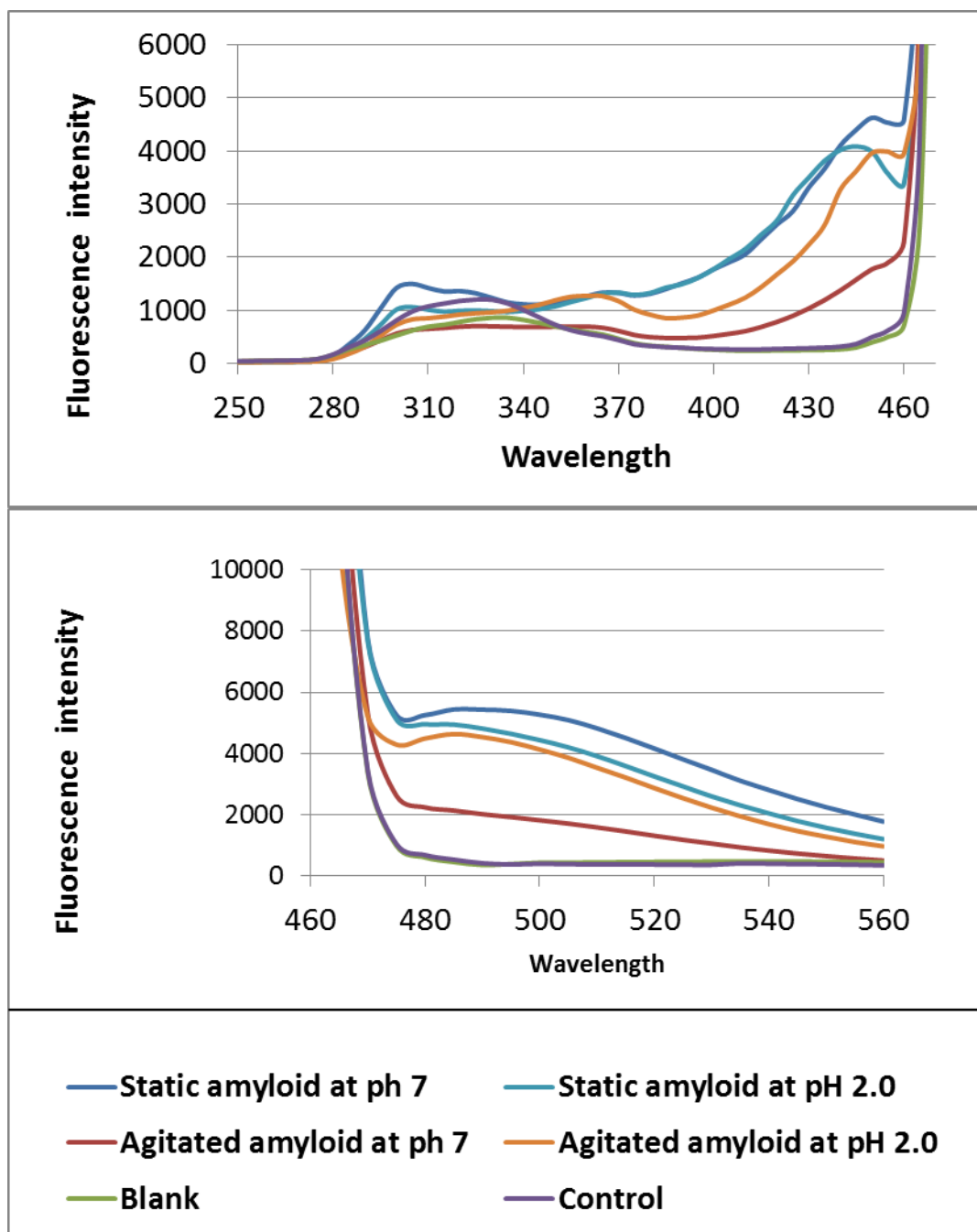
Figure 3.14: ThT excitation and emission spectra of HEWL amyloid aggregates at pH 2.0 & 7.0

Furthermore, we examined the dis-aggregation of the two types of amyloid aggregates by the potent chaotroph urea which is well known to denature proteins by breaking hydrophobic interactions. Consistent with the pH dis-aggregation data, the static amyloid aggregates showed greater urea stability as well, as compared with the agitated

amyloid aggregates **(Figure 3.15)**. This further indicates that the conformations of the two amyloids are different.
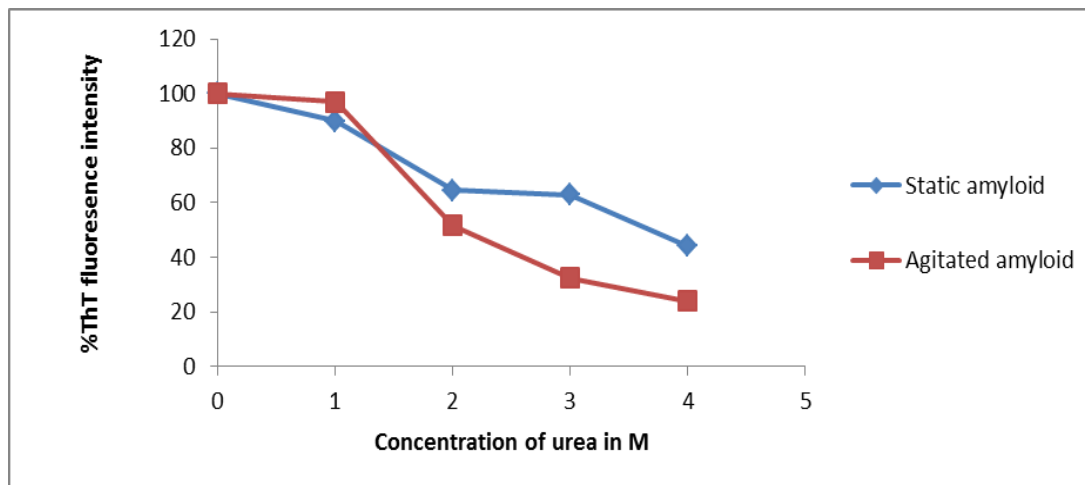

Figure 3.15: Stability of amyloids towards increasing concentration of denaturant urea

3.7. ENZYME ACTIVITY ASSAY OF SOLUBLE HEWL AND ITS AMYLOID FORMS

When the agitated and static amyloids pre-fibrillized at pH 2.0 are shifted to pH 7.0 for lysozyme activity, only the agitated aggregates regain lysozyme activity which could be either because of release of monomers from the aggregates or due to presence of monomers in the fibrillized samples if all protein monomers had not joined the aggregates **(Figure 3.16)**. However, the possibility that the lysozyme molecules even after joining the aggregates formed by agitation (which are relatively short size aggregates) may retain the activity cannot be ruled out.
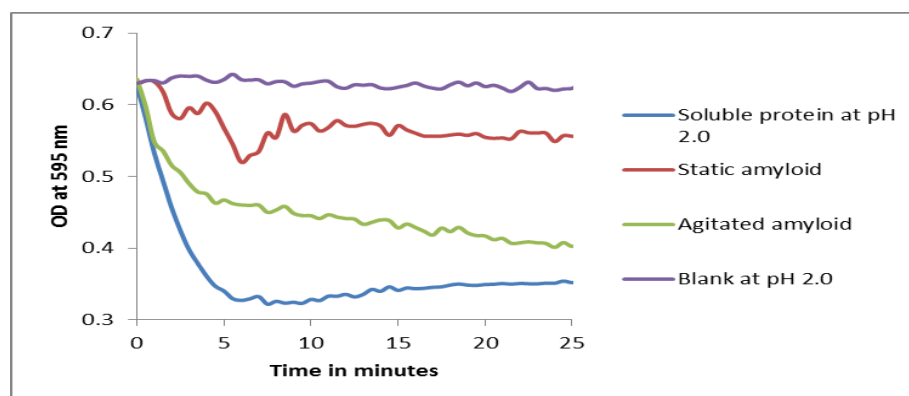

Figure 3.16: Enzyme activity kinetics of soluble HEWL and amyloid forms

51

CHAPTER IV

CONCLUSION

Conclusion

Hen Egg White Lysozyme is a good model protein, being easily available and is well characterized, both enzymatically and structurally. The results can be correlated to *in vivo* lysozyme amyloidosis since HEWL shows 60% sequence identity with human lysozyme and it also displays a large degree of structural homology with human lysozyme.

From the Thioflavin T fluorescence and Congo red binding assays it is clear that HEWL can be induced to form amyloid at low pH of 2.0 and at 37 °C. Kinetic results show that the presence of agitation increases the rate of formation of amyloid.

Analysis of seeding and conformational cross seeding indicates the formation of conformational variants in the presence and absence of agitation during fibrillization. While the self-seeding was efficient when the static amyloid seeds were used to seed static incubated monomers (or if the agitated amyloid seeds were used to seed the agitated monomers), the cross-seeding of agitated monomers by static amyloid seed (or the cross-seeding of static monomers by agitated amyloid seed) was not observed (Figure 3.7-3.10). The presence of variant conformation is further and strongly supported by the observation that the two types of amyloids show different sizes of detergent (sarkosyl)-resistant particles and also exhibit different stabilities against pH and urea. Taken together, here we succeeded in generating self-propagating amyloid variants of HEWL amyloid aggregates, a finding that could have relevance to the human lysozyme amyloidosis.
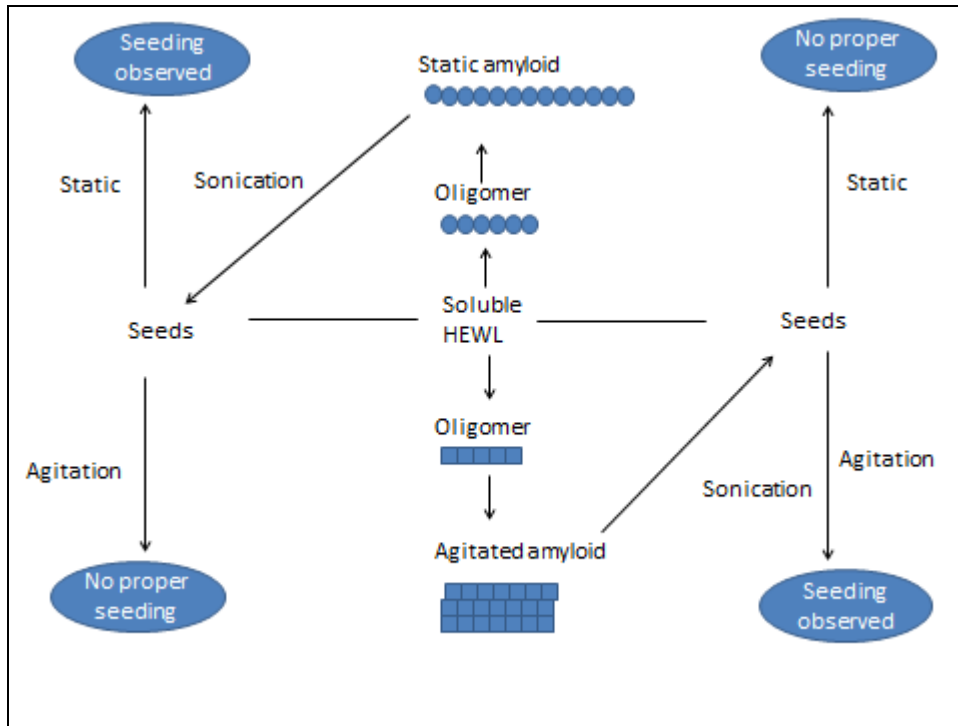
Figure 3.17: Summary of observations on seeding & conformational cross-seeding of HEWL amyloid aggregates

CHAPTER V

REFERENCES

REFERENCES

1. Kyle, R.A., *Amyloidosis: a convoluted story.* Br J Haematol, 2001. **114**(3): p. 529-38.

2. Dobson, C.M., *The structural basis of protein folding and its links with human disease.* Philos Trans R Soc Lond B Biol Sci, 2001. **356**(1406): p. 133-45.

3. Chiti, F. and C.M. Dobson, *Protein misfolding, functional amyloid, and human disease.* Annu Rev Biochem, 2006. **75**: p. 333-66.

4. Eisenberg, D. and M. Jucker, *The amyloid state of proteins in human diseases.* Cell, 2012. **148**(6): p. 1188-203.

5. Sunde, M. and C.C. Blake, *From the globular to the fibrous state: protein structure and structural conversion in amyloid formation.* Q Rev Biophys, 1998. **31**(1): p. 1-39.

6. Mankar, S., et al., *Nanomaterials: amyloids reflect their brighter side.* Nano Rev, 2011. **2**.

7. Fowler, D.M., et al., *Functional amyloid formation within mammalian tissue.* PLoS Biol, 2006. **4**(1): p. e6.

8. Astbury, W.T., S. Dickinson, and K. Bailey, *The X-ray interpretation of denaturation and the structure of the seed globulins.* Biochem J, 1935. **29**(10): p. 2351-2360 1.

9. Eanes, E.D. and G.G. Glenner, *X-ray diffraction studies on amyloid filaments.* J Histochem Cytochem, 1968. **16**(11): p. 673-7.

10. Nelson, R., et al., *Structure of the cross-beta spine of amyloid-like fibrils.* Nature, 2005. **435**(7043): p. 773-8.

11. Rambaran, R.N. and L.C. Serpell, *Amyloid fibrils: abnormal protein assembly.* Prion, 2008. **2**(3): p. 112-7.

12. Krebs, M.R., et al., *Observation of sequence specificity in the seeding of protein amyloid fibrils.* Protein Sci, 2004. **13**(7): p. 1933-8.

13. Kumar, S. and J. Walter, *Phosphorylation of amyloid beta (Abeta) peptides - a trigger for formation of toxic aggregates in Alzheimer's disease.* Aging (Albany NY), 2011. **3**(8): p. 803-12.

14.   Bessen, R.A. and R.F. Marsh, *Identification of two biologically distinct strains of transmissible mink encephalopathy in hamsters.* J Gen Virol, 1992. **73 (Pt 2)**: p. 329-34.

15.   Bessen, R.A. and R.F. Marsh, *Distinct PrP properties suggest the molecular basis of strain variation in transmissible mink encephalopathy.* J Virol, 1994. **68**(12): p. 7859-68.

16.   Pepys, M.B., *Amyloidosis.* Annu Rev Med, 2006. **57**: p. 223-41.

17.   Cobb, N.J. and W.K. Surewicz, *Prion diseases and their biochemical mechanisms.* Biochemistry, 2009. **48**(12): p. 2574-85.

18.   Prusiner, S.B., *Novel proteinaceous infectious particles cause scrapie.* Science, 1982. **216**(4542): p. 136-44.

19.   Fowler, D.M., et al., *Functional amyloid--from bacteria to humans.* Trends Biochem Sci, 2007. **32**(5): p. 217-24.

20.   Liebman, S.W. and I.L. Derkatch, *The yeast [PSI+] prion: making sense of nonsense.* J Biol Chem, 1999. **274**(3): p. 1181-4.

21.   Tanaka, M., et al., *Conformational variations in an infectious protein determine prion strain differences.* Nature, 2004. **428**(6980): p. 323-8.

22.   Tanaka, M., et al., *The physical basis of how prion conformations determine strain phenotypes.* Nature, 2006. **442**(7102): p. 585-9.

23.   Petkova, A.T., et al., *Solid state NMR reveals a pH-dependent antiparallel beta-sheet registry in fibrils formed by a beta-amyloid peptide.* J Mol Biol, 2004. **335**(1): p. 247-60.

24.   Tycko, R., *Solid-state NMR studies of amyloid fibril structure.* Annu Rev Phys Chem, 2011. **62**: p. 279-99.

25.   Swaminathan, R., et al., *Lysozyme: a model protein for amyloid research.* Adv Protein Chem Struct Biol, 2011. **84**: p. 63-111.

26.   Canfield, R.E., *The Amino Acid Sequence of Egg White Lysozyme.* J Biol Chem, 1963. **238**: p. 2698-707.

27.   Morozova-Roche, L.A., et al., *Amyloid fibril formation and seeding by wild-type human lysozyme and its disease-related mutational variants.* J Struct Biol, 2000. **130**(2-3): p. 339-51.

28. Booth, D.R., et al., *Instability, unfolding and aggregation of human lysozyme variants underlying amyloid fibrillogenesis.* Nature, 1997. **385**(6619): p. 787-93.

29. Granel, B., et al., *Lysozyme amyloidosis: report of 4 cases and a review of the literature.* Medicine (Baltimore), 2006. **85**(1): p. 66-73.

30. Sattianayagam, P.T., et al., *Hereditary lysozyme amyloidosis -- phenotypic heterogeneity and the role of solid organ transplantation.* J Intern Med, 2012. **272**(1): p. 36-44.

31. Granel, B., et al., *Recurrent hepatic hematoma due to familial lysozyme amyloidosis resolves with conservative management.* Amyloid, 2014. **21**(1): p. 66-8.

32. McCarthy, C., et al., *Combined pulmonary involvement in hereditary lysozyme amyloidosis with associated pulmonary sarcoidosis: a case report.* Sarcoidosis Vasc Diffuse Lung Dis, 2013. **30**(4): p. 321-4.

33. Gillmore, J.D., et al., *Hereditary renal amyloidosis associated with variant lysozyme in a large English family.* Nephrol Dial Transplant, 1999. **14**(11): p. 2639-44.

34. Tokunaga, Y., et al., *Analysis of core region from egg white lysozyme forming amyloid fibrils.* Int J Biol Sci, 2013. **9**(2): p. 219-27.

35. Biancalana, M. and S. Koide, *Molecular mechanism of Thioflavin-T binding to amyloid fibrils.* Biochim Biophys Acta, 2010. **1804**(7): p. 1405-12.

36. LeVine, H., 3rd, *Thioflavine T interaction with synthetic Alzheimer's disease beta-amyloid peptides: detection of amyloid aggregation in solution.* Protein Sci, 1993. **2**(3): p. 404-10.

37. Khurana, R., et al., *Mechanism of thioflavin T binding to amyloid fibrils.* J Struct Biol, 2005. **151**(3): p. 229-38.

38. Klunk, W.E., J.W. Pettegrew, and D.J. Abraham, *Quantitative evaluation of congo red binding to amyloid-like proteins with a beta-pleated sheet conformation.* J Histochem Cytochem, 1989. **37**(8): p. 1273-81.

39. Kryndushkin, D.S., et al., *Yeast [PSI+] prion aggregates are formed by small Sup35 polymers fragmented by Hsp104.* J Biol Chem, 2003. **278**(49): p. 49636-43.

40.   Bagriantsev, S. and S.W. Liebman, *Specificity of prion assembly in vivo. [PSI+] and [PIN+] form separate structures in yeast.* J Biol Chem, 2004. **279**(49): p. 51042-8.